UNIVERSITEIT VAN PRETORIA
UNIVERSITY OF PRETORIA
YUNIBESITHI YA PRETORIA

Denkleiers • Leading Minds • Dikgopolo tša Dihlalefi

Assessing the role of the KISS1 receptor in breast cancer behaviour with the use of CRISPR-mediated gene editing

By

Alex Leah Marais

Submitted in partial fulfilment of the requirements for the Master of Science degree in

Human Physiology

in the

Department of Physiology

Faculty of Health Sciences

UNIVERSITY OF PRETORIA

2023

Abstract

The recent advancements in gene editing have provided scientists with a powerful tool for the investigation of the role of individual proteins in cellular physiology and disease. Gene editing was preceded by another powerful technology that changed cell biology, short hairpin ribonucleic acid (shRNA) dependent messenger RNA (mRNA) degradation. In this project, we sought to establish cell lines derived from the triple negative breast cancer (TNBC) cell line, MDA-MB-231, that expressed low or no Kisspeptin receptor (KISS1R) protein. KISS1R is the cognate receptor of a peptide called kisspeptin. Our previous studies have shown that KISS1R is expressed in different TNBC cell lines but responds differently to a kisspeptin derivative, kisspeptin-10 (KP-10). Using a cell line with low or no KISS1R expression, we can further investigate this phenomenon of alternative signalling to understand the potential role of KISS1R in breast cancer biology. Here, we first established an MDA-MB-231 cell line stably expressing KISS1R shRNA through lentiviral vector delivery and show that while we reduce *KISS1R* mRNA levels by more than 90%, enough protein remains to allow for a functional response to KP-10 in the form of calcium release. Subsequently, we established a Clustered Regularly Interspaced Short Palindromic Repeats (CRISPR)-mediated gene editing strategy using HEK-293T cells as a model cell line after which we used electroporation and single cell sorting to establish clonal lines with insertion-deletion mutations (INDELs) for KISS1R. Our efforts have resulted in the establishment of several clones of HEK-293T and MDA-MB-231 cells with no wildtype alleles and frameshifts or large deletions in the KISS1R gene. These can now be used for direct functional studies of KISS1R in TNBC.

Key words: Gene editing, CRISPR-Cas9, breast cancer, TNBC, HEK-293T, MDA-MB-231, kisspeptin, KISS1R, calcium

Declaration

I hereby declare that the work presented in this dissertation for the degree Master of Science in Human Physiology is my work and has not been submitted for any other degree either at the University of Pretoria or another university.

Signed:

Alex L. Marais

Acknowledgements

This project would not have been possible without the guidance and support of my supervisor, Dr Iman van den Bout. We might not have always seen eye to eye but I am grateful that you have always pushed me to do more and to be a better scientist. To my co-supervisor, Dr Ross Anderson, thank you for your guidance and support.

To Dr Felicia Azubuike, thank you for taking the time to train and teach me. Learning from you was an honour, and I can't wait to see where your career takes you next. To the remaining members of the CNE, thank you for all the assistance you have provided through this research study.

To my family, thank you for all the love and support that you have given me over my academic career. It hasn't always been easy, but we have always overcome whatever difficulties life has thrown at us, together.

To Dr Chrisna Durandt and Jamie Mollentze, thank you for the assistance provided with flow cytometry and cell sorting. Your assistance was vital in obtaining these results.

To my partner in crime, Mandy, thank you for your support this past year. The late nights and early mornings were always more bearable with you around. Thank you for always challenging me and pushing me to be the best version of myself.

This project was supported by an Innovation bursary from the National Research Foundation

Table of Contents

List of Figures

List of Tables

List of Abbreviations

ACTB	β-actin
AML	Acute myeloid leukaemia
BAALC	Brain and acute leukaemia cytoplasmic protein
Bp	Base pairs
BCA	Bicinchoninic acid
BSA	Bovine serum albumin
Cas9	CRISPR associated protein 9
cAMP	Cyclic adenosine monophosphate
cDNA	Complementary deoxyribonucleic acid
CMV	Cytomegalovirus
CRISPR	Clustered Regularly Interspaced Palindromic Repeats
crRNA	CRISPR RNA
CXCR4	C-X-C chemokine receptor type 4
CXCR7	C-X-C chemokine receptor type 7
DAG	Diacylglycerol
DMEM	Dulbecco's Modified Eagle Medium
DMSO	Dimethyl Sulphoxide
DNA	Deoxyribonucleic acid
E. Coli	*Escherichia coli*
EDTA	Ethylenediaminetetraacetic acid
ER	Endoplasmic Reticulum
ERα	Oestrogen receptor α
FASN	Fatty acid synthase
FBS	Fetal Bovine Serum
gDNA	Genomic Deoxyribonucleic acid
GFP	Green Fluorescent Protein
GDP	Guanine diphosphate
GnRnH	Gonadotrophin-releasing hormone
GPCR	G-protein coupled receptor
GPR54	G-protein receptor 54
GRK	G-protein coupled receptor kinases
GTP	Guanine triphosphate
HBSS	Hank's balanced salt solution
HCl	Hydrochloric acid
HDR	Homology-directed repair
HEK-293T	Human Embryonic Kidney cell
HER2	Human epidermal growth factor 2
HIV	Human Immunodeficiency Virus
HNH	Homing endonuclease
HPG	Hypothalamic-pituitary-gonadal
HRP	Horseradish Peroxidase
IP_3	Inositol 1,4,5-triphosphate
KO	Knockout
KP	Kisspeptin
KISS1R	KISS1 receptor
KP-54	Kisspeptin-54
KP-14	Kisspeptin-14
KP-13	Kisspeptin-13
KP-10	Kisspeptin-10
LB Broth	Luria-Bertani broth
MAPK	Mitogen-activated protein kinase
MMP	Matrix metalloproteases
mRNA	Messenger RNA
NGS	Next generation sequencing
NHEJ	Non-Homologous End Joining
NSC	Neural stem cell

nTPM	Normalized Transcript Expression Value
ORF	Open Reading Frame
OSR1	Oxidative Stress-Responsive kinase 1
PAM	Protospacer adjacent motif
PBS	Phosphate-buffered Saline
PDGF	Platelet-derived growth factor
PEI	Polyethylenamine
PIP_2	Phosphatidylinositol 4,5-bisphosphate
PVDF	Polyvinylidene Difluoride
PCR	Polymerase Chain Reaction
PR	Progesterone receptor
RIPA	Radioimmunoprecipitation
RH	Relative humidity
RhoGEF	Rho guanine-nucleotide exchange factor
RNA	Ribonucleic acid
RT	Reverse Transcriptase
SCD	Sickle cell disease
SDS	Sodium Dodecyl Sulphate
SERD	Selective oestrogen receptor modulator
SFM	Serum-free media
sgRNA	Single guide Ribonucleic acid
shRNA	Small hairpin Ribonucleic acid
SPAK	Ste20- and SPS1-related proline alanine-rich kinase
S. pyrogenes	*Streptococcus pyogenes*
SRSR	Short Regularly Spaced Repeats
TALEN	Transcription Activator-like Effector Nucleases
TCR	T cell receptor
TNBC	Triple negative breast cancer
TracrRNA	Trans-activating CRISPR RNA
WHO	World Health Organization
ZFN	Zinc Finger Nucleases

Chapter 1: Introduction

1.1 Genome editing

The recent advances in genome editing, also known as gene editing, have enabled new possibilities in the treatment of diseases, such as cancer and Human Immunodeficiency Virus (HIV).[1] Before the discovery of the Clustered Regularly Interspaced Short Palindromic Repeats (CRISPR) -CRISPR-associated protein (Cas) system, scientists developed Zinc-Finger Nucleases (ZFNs) and Transcription Activator-like Effector Nucleases (TALENs), which are reprogrammed nucleases that when combined with a deoxyribonucleic acid (DNA) binding domain, induce double-stranded breaks (DSBs) in DNA at target sites (Figure 1.1).[2,3] DNA repair then either occurs through two mechanisms; Non-Homologous End Joining (NHEJ) or Homology-directed repair (HDR). While HDR will repair the site using the second allele of the gene as a template thus generating a perfect fix, NHEJ will repair the break without a template resulting in the insertion or deletion of nucleotides. NHEJ will thus result in different effects including insertions of stop codons, frameshift or missense mutations.[4–6]

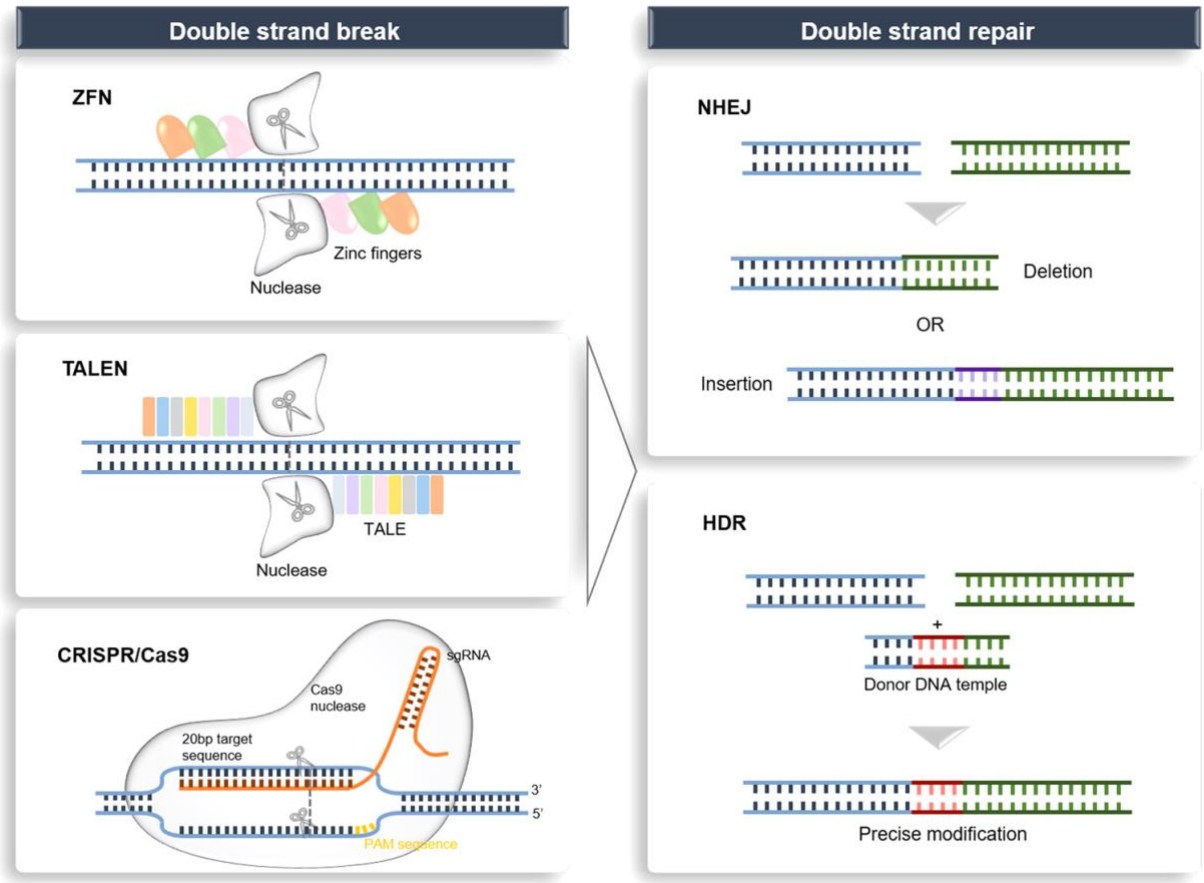

Figure 1.1: Diagram depicting the current gene editing technologies available.

The image depicts the different technologies available to introduce targeted double stranded DNA breaks, which will be repaired by the host cells through either non-homologous end joining (NHEJ) causing insertion-deletion (INDEL) mutations or through homology directed repair (HDR) which will generate a perfect fix. Transcription Activator-like Effector Nucleases (TALENs) and the Clustered Regularly Interspaced Short Palindromic Repeats (CRISPR)-CRISPR associated protein (Cas) 9 system are currently at the forefront of gene editing technology. Image reproduced from Li *et al* with permission from Springer Nature.[7]

1.2 CRISPR-Cas9 gene-editing

While TALEN and ZFN technology were revolutionary, their cost and low efficiency prohibited them from mainstream scientific use. In contrast, CRISPR-Cas9 delivers on all these aspects to make this a truly revolutionary tool for scientists.

1.2.1 History

The first CRISPR sequence was described in 1986 in *Escherichia coli*, but it was only in 2000 when Mojica *et al* characterised short palindromic repeats interspaced by unique intervening sequences, found in archaea, bacteria and mitochondria genomes, that a family of sequences known as Short Regularly Spaced Repeats (SRSRs) was recognised.[8] Through the sequencing of multiple organisms, it was discovered that these sequences were highly conserved within members of the same phylogenetic tree, as well as between domains, which suggested biological importance.[9]

In 2002, through comparison of SRSRs (renamed CRISPR)-containing prokaryotes and CRISPR-free prokaryotes, 4 CRISPR-associated (Cas) genes were identified.[10] Two years later, researchers in France studying *Yersinia pestis* identified homology of these spacer sequences with bacteriophage DNA, confirming the speculation that the CRISPR and Cas genes played an important role in bacterial immunity.[11] Researchers expanded on this understanding by identifying that most spacer regions are derived from bacteriophages, while others are derived from other extrachromosomal sources such as plasmids. These researchers also provided evidence that correlated sensitivity of *Streptococcus thermophillus* to bacteriophages with the number of spacers found between the repeats. They suggested that transcription of these sequences produced anti-sense Ribonucleic acid (RNA) that facilitated degradation of foreign DNA.[12,13] Even though more evidence was found that proved that CRISPR played an important role in prokaryote adaptive immunity, they still did not understand how this was done.[14]

In 2012, Jinek *et al* published an article that described the role of CRISPR sequences and Cas genes in prokaryotic immunity.[15] Prokaryotic adaptive immunity occurs in three steps; after exposure to a virus or plasmid, short fragments of the foreign sequences are integrated into the spacer sequences between CRISPR. The transcription of these foreign sequences results in pre-cursor CRISPR RNA (crRNA), and following cleavage, mature crRNA are produced that binds to the complementary sequences on the invading virus or plasmid. This

recognition combined with Cas endonucleases results in the destruction of the virus or plasmid.

These scientists identified three different types of CRISPR-Cas systems based on their mechanisms. The type I and III systems have similar features; specialized Cas endonucleases process pre-cursor crRNA to mature crRNA. Each mature crRNA assembles with a multi-subunit of Cas endonucleases, which recognises and cleaves DNA complementary to the crRNA. In contrast, the type II CRISPR-Cas system requires a trans-activating crRNA (tracrRNA) to initiate the processing of the pre-cursor crRNA. When required, the tracrRNA and pre-cursor crRNA are transcribed. The tracrRNA recruits the endoribonuclease RNase III and the Cas9 protein to the pre-cursor crRNA initiating processing, resulting in a mature crRNA and tracrRNA attached to a Cas9 protein.[16–18]

Off of this mechanism, the same scientists were able to show that a single guide RNA (sgRNA) combining the functional parts of the crRNA and tracrRNA could be used to guide the Cas9 protein to a specific gene and induce a DSB, making this discovery a large advancement in gene editing.[15]

1.2.2 Mechanism

Cas9 endonuclease has been shown to have a domain similar to Homing (HNH) endonucleases and another similar to RuvC endonucleases, which are responsible for inducing DSBs in DNA. In order for cleavage to occur, the appropriate protospacer adjacent motif (PAM) is required for the Cas9 protein to recognise its target.[15,19] As indicated in Figure 1.2, the PAM sequence is located upstream from the site of interest and cleavage occurs three nucleotides downstream of the PAM sequence. Once a DSB has occurred, DNA will be repaired either through HDR or NHEJ.[20] HDR uses the same allele on the sister chromatid as a template to ensure that the gene is correctly repaired to its previous form.[6] NHEJ is the imperfect form of repair since it does not make use of a template, which can result in the insertion or deletion of nucleotides. These insertion and deletions (INDELs) have the ability to shift the reading frame (called a frameshift mutation) resulting in either the absence of the protein or the production of an abnormal protein. [5]

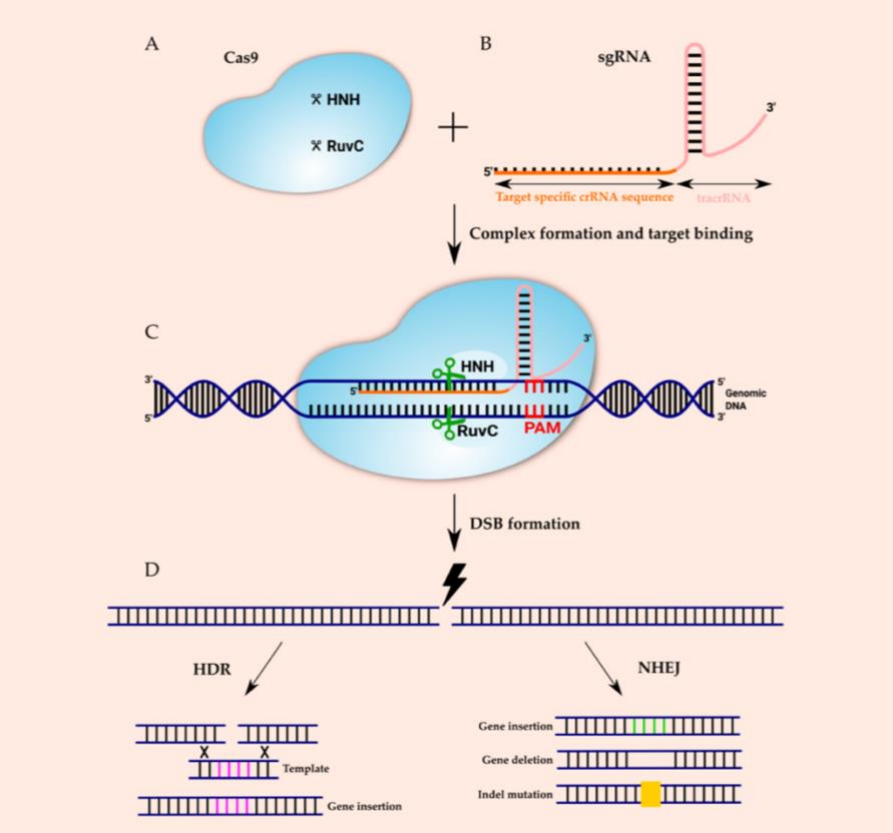

Figure 1.2: A schematic diagram depicting the mechanism by which CRISPR-Cas9 generates double stranded DNA breaks inducing the formation of INDEL mutations.

(A) Cas9 contains two endonuclease motifs similar to HNH and RuvC endonucleases which enable DSBs. (B) A single guide RNA (sgRNA) contains a targeting sequence which corresponds to the DNA sequence of interest and a tracrRNA sequence containing a PAM sequence which allows it to bind the Cas9 protein to the genomic DNA. Cas9 recognises the PAM sequences and causes a DSB downstream from the sequence. (D) The DNA is then repaired either through HDR or NHEJ. Image reprinted from Janik *et al* with permission from MDPI. [20]

1.2.3 Applications

Prior to the landmark 2012 paper, gene therapy for autoimmune disorders and cancer had already started to gain momentum. The premise being that if a protein is defective or absent, the protein can simply be administered to the patients. Between 1998 and 2019, 22 gene therapies had already been approved by the regulatory bodies of various countries, a few of these being CRISPR-Cas9 based therapies.[21]

In 2020, phase I clinical trials were initiated to test CRISPR-Cas9 edited T cells that had both T cell chain genes (T cell receptor α and β) and its programmed cell death protein 1 (PD-1) deleted. The T cells were then infected with lentivirus containing DNA for a specialised T cell receptor (TCR) transgene that is specific for cancer cells. These specialised T cells were then transfused back into the patients who were not responding to other therapies.[1]

CRISPR-Cas9 technology has also created new opportunities in the treatment of Sickle cell disease (SCD), which is monogenic disorder caused by a missense mutation in the β-globin gene resulting in the production of an abnormal form of haemoglobin.[22] In 2020, the first CRISPR-Cas9 treatment of SCD and transfusion-dependent β-Thalassemia on two patients was reported. The patients received transfusions of autologous CD34+ Haematopoietic stem cells with the gene, BCL11A silenced. BCL11A is a transcription factor responsible for the repression of haemoglobin F (the foetal form of haemoglobin). A year later, both patients displayed high levels of allelic editing in the bone marrow and blood, an increase in foetal haemoglobin, transfusion independence and elimination of symptoms experienced by the patient with SCD.[23] While the CRISPR-Cas9 system has already shown its usefulness in treating diseases, it is also a tool that scientists can use in laboratory research.

1.3 G-protein coupled receptors

The G-protein coupled receptor (GPCR) family is the largest family of proteins in the human genome with approximately 800 receptors reported.[24] GPCRs have a wide range of physiological roles, including olfaction, neurotransmission, metabolism and growth, and respond to an even wider variety of endogenous and exogenous signals.[25] Approximately, 460 GPCRs have been shown to recognise odorants and play a role in olfaction while others recognise and respond to hormones, light, metabolites and neurotransmitters.[26] While the endogenous ligands of the majority of GPCRs are known, the endogenous ligands of more than 100 of these receptors (named orphan receptors) remain unknown.[27] Identifying the functions and the associated ligands of the orphan receptors is vital as this is an untapped area of research that could assist in the development of drug therapies. Currently, 35% of all drugs approved by the Food and Drug Administration (FDA) target only 134 GPCRs.[28]

1.3.1 Structure

While GPCRs can differ greatly in their functions, they all display a similar structure. The first discovery that gave insight into the structure of GPCRs came in the early 1990's, where the structure of the hamster β2 adrenergic receptor, bovine rhodopsin and *Saccharomyces cerevisiae* α-factor (STE2 gene) were compared. It was shown that all three receptors had a 7 transmembrane region with alternating extracellular and intracellular loops (ECL and ICL respectively) (Figure 1.3.).[29,30] Since then, there has been a great effort to determine the primary sequences of more GPCRs, resulting in the identification of 800 different receptors.[31]

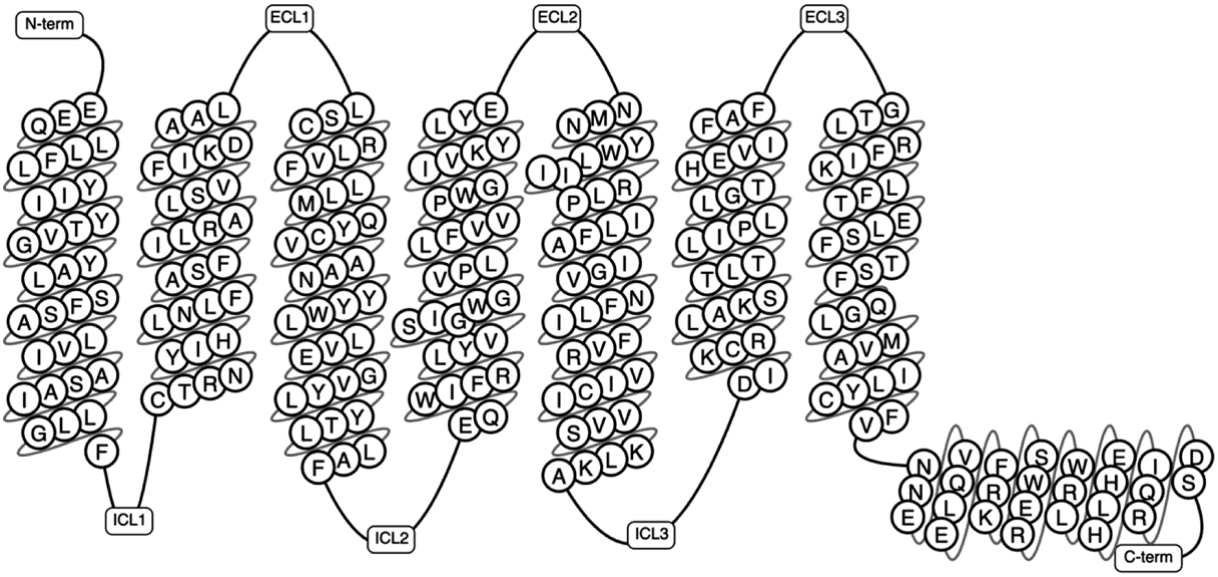

Figure 1.3: Basic amino acids sequence and structure of KISS1R.

The basic structure of any GPCR includes a extracellular N-terminus attached to 7 transmembrane regions separated by extracellular and intracellular loops ending in an intracellular C-terminus of variable length. Class A GPCRs have an 8th helix that lies parallel to the membrane. N-term: N-terminus; C-term: C-terminus; ECL: Extracellular region; ICL: Intracellular region. Image reprinted from Odoemelam *et al* with permission from the Royal Society of Chemistry. [32]

GPCRs have been subdivided into five different families namely, the rhodopsin, glutamate, secretin, adhesion and frizzled/taste2 families through phylogenetic analysis based on conserved sequences,.[26,33] The rhodopsin family is the largest family comprising of approximately 680 members and has been further subdivided into 4 groups - α, β, γ and δ, with a further 13 subdivisions.[34] As the name suggests, GPCRs are associated with a heterotrimeric G-protein consisting of an α subunit, that harbours GTPase activity and binds guanine nucleotides, and a $\beta\gamma$ dimer. By 2002, researchers had cloned 16 Gα, 5 Gβ and 12 Gγ subunits.[31,35] G-proteins are named after their Gα subunits, therefore a Gs protein will have a Gαs subunit and a Gq protein will have a Gαq subunit. [31] When activated, the Gα and G$\beta\gamma$ sub-units initiate different downstream signals as highlighted by Table 1.1.

1.3.2 Signalling

When a GPCR is in its inactive state, the α subunit is bound to guanine diphosphate (GDP) and complexed with a $\beta\gamma$ dimer. After the receptor is activated, the receptor undergoes a conformational change increasing its affinity for G-proteins. The heterotrimeric G-protein couples with the receptor, causing GDP to be released and exchanged for a guanine triphosphate (GTP). This change causes the Gα protein to dissociate from the GPCR and the $\beta\gamma$ dimer, with both subunits going on to initiate various downstream signalling pathways (Figure 1.4).[35,36] Depending on the Gα subunit, dissociation of the G-protein can result in either

the stimulation or inhibition of adenylyl cyclase or the activation of Phospholipase C-β. Table 1.1 highlights the Gα subunits, as well as the Gβγ dimer, and the downstream effects they have after activation.[36] After initiating downstream signalling, the Gα subunit hydrolyses GTP resulting in its conversion to GDP. The Gα subunit reassociates with the βγ dimer and awaits further activation.

Table 1.1: The different G-protein subunits and the proteins they interact with after activation.

G-protein subunit	Result of activation
$G\alpha_s$	Activates adenylyl cyclase 1-9[37,38]
$G\alpha_q$	Activates Phospholipase C-β 1/3/4 [39]
$G\alpha_{q/11}$	Activates Phospholipase C-β 1/3/4 [39]
$G\alpha_{i1}$	Inhibits adenylyl cyclase 1/5/6 [37,38,40]
$G\alpha_{t\text{-}cone}$	Activates Phosphodiesterase 6 [37,38,40]
$G\alpha_{12}$	Activates Rho guanine nucleotide exchange factor[41]
Gβγ	Activates adenylyl cyclase [42] Activates phospholipase C [43] Activates G-protein regulated inwardly rectifying potassium channel [44] Activates phosphatidylinositol-3 kinase [45]

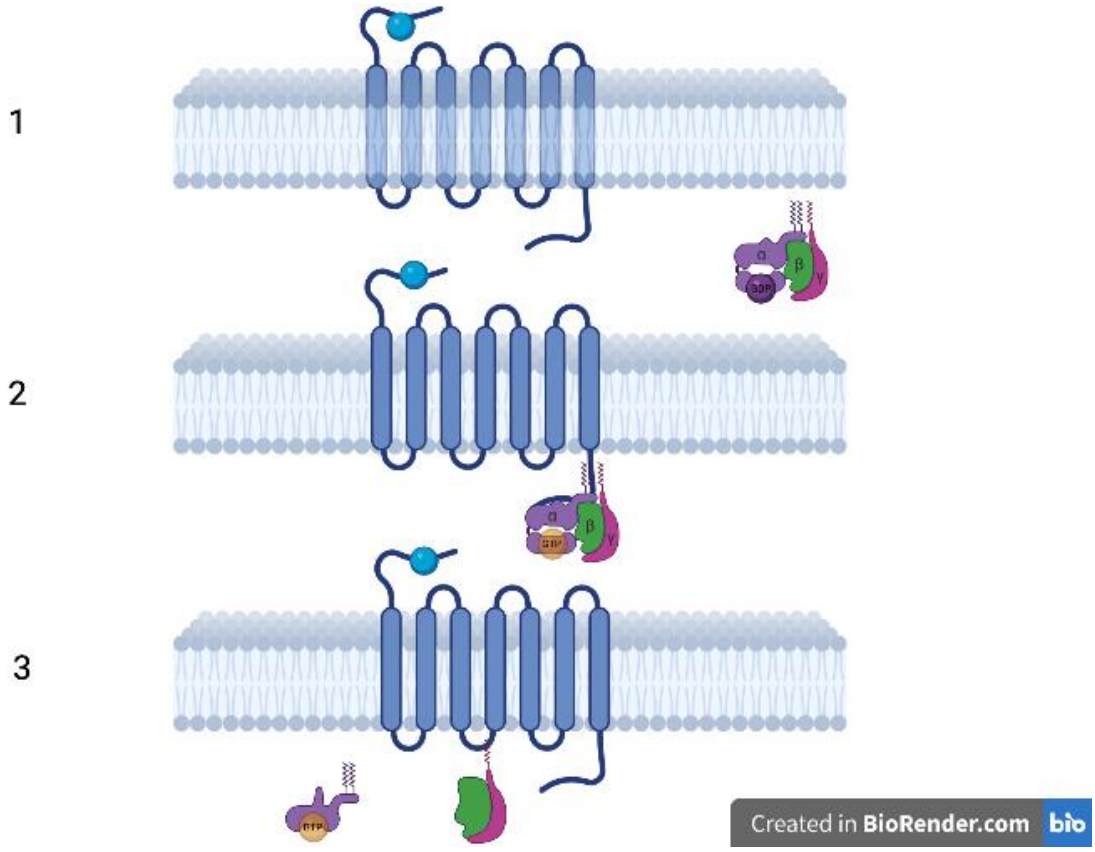

Figure 1.4: Diagram depicting the changes in GPCR conformation and binding after activation by a ligand.

(1 and 2) After ligand binding the GPCR changes its conformation resulting in the attraction of an inactive G-protein trimer and the exchange of GDP for GTP. (3) The exchange of GDP for GTP causes the G-proteins to dissociate into a Gα subunit and Gβγ dimer with each component enabled to direct further downstream signalling. Image created using BioRender.com

1.3.3 G-protein dependent signalling

When activated the different subunits impact different downstream pathways providing complexity in the system (Figure 1.5). For instance, $G\alpha_s$ stimulates adenylyl cyclase which increases the production of cyclic adenosine monophosphate (cAMP). Due to the rising levels of cAMP, protein kinase A is activated which phosphorylates cellular proteins that promote transcription of genes. When activated, $G\alpha_i$ inhibits adenylyl cyclase, reducing the levels of intracellular cAMP.[31,46] The $G\alpha_{q/11}$ protein family activates phospholipase C-β which is responsible for converting phosphatidylinositol 4,5-bisphosphate (PIP_2) to inositol 1,4,5-triphosphate (IP_3) and diacylglycerol (DAG), as well as activating the protein kinase B (AKT/PKB) signalling pathway. IP_3 binds to IP_3 receptors in the endoplasmic reticulum (ER) resulting in the release of calcium, and DAG activates protein kinase C, which activates extracellular signal-regulated kinases (ERK) 1/2, which forms part of the Mitogen activated protein kinase (MAPK) pathway.[47] The $G\alpha_{12/13}$ protein family activates the GTPase enzyme Rho by activating Rho guanine-nucleotide exchange factors (RhoGEFs). RhoGEFs are responsible for the release of GDP from Rho and the subsequent binding of GTP resulting in its activation.[41,48] Activation of all these downstream signals initiate the expression of genes required for cell proliferation, migration and angiogenesis.[49,50]

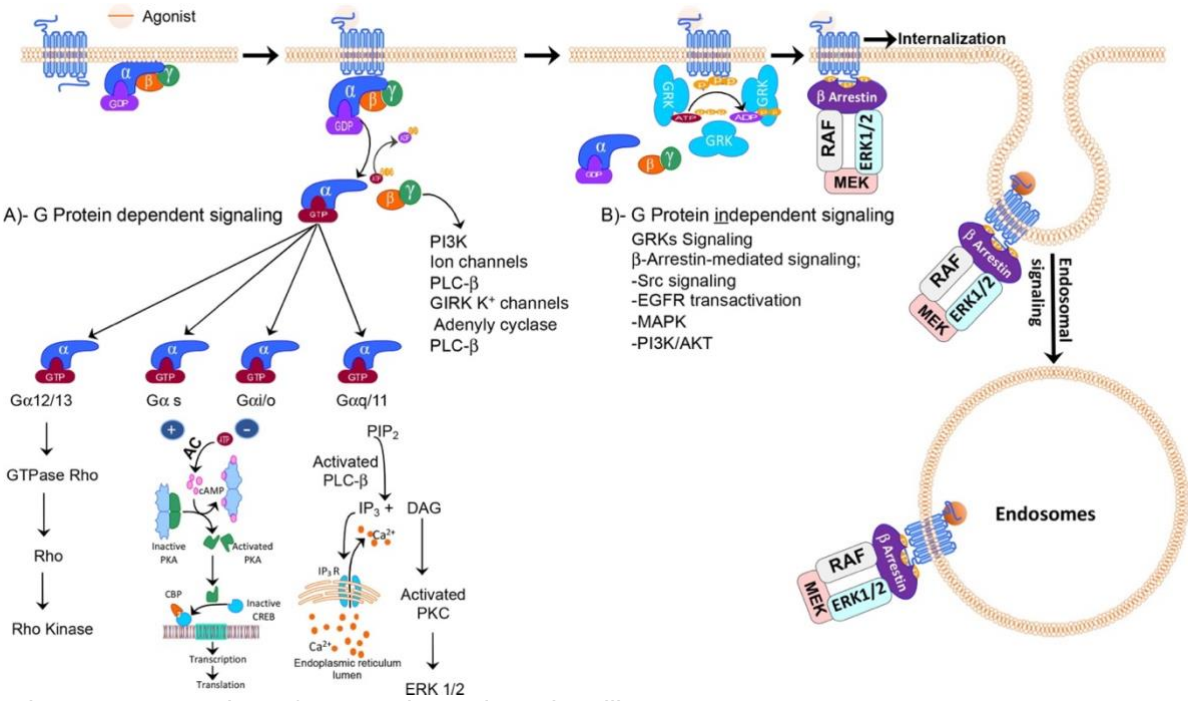

Figure 1.5: Overview of GPCR dependent signalling.

The image depicts the major avenues of signalling elicited by GPCR activation through the activation of different G-proteins as well as alternative downstream signalling mediators such as arrestins. Image reproduced from Alhosaini *et al* with permission from Elsevier.[46]

1.3.4 G-protein independent signalling

While most GPCRs signal through G-protein dependent pathways, downstream signalling can also occur through G-protein independent pathways. G-protein coupled receptor kinases (GRKs) and β-arrestin 1/2 were first shown to play an important role in receptor desensitisation and internalisation.[51,52] After activation of the GPCR, GRKs phosphorylate serine/threonine residues at the C-terminus, resulting in the recruitment of β-arrestin 1/2 thus preventing the binding of the heterotrimeric G-protein, and facilitating clathrin-mediated endocytosis. GRKs have been shown to interact with other proteins such as R-SMAD, p58 and platelet-derived growth factor (PDGF), while β-arrestin 2 has been shown to activate the ERK (MAPK) pathway.[53,54,55] The GPCR of interest in this study is KISS1R.

1.4 Kisspeptin and KISS1R

1.4.1 Kisspeptin

In 1996, the KISS-1 gene, which was later found to encode kisspeptin (KP), was identified as a metastasis suppressor since its absence was correlated with metastasis in melanoma cells.[56] Kisspeptin encodes a 145 amino acid precursor known as pre-prokisspeptin, which is further cleaved by matrix metalloproteases (MMPs) to different forms of kisspeptin of varying amino acid lengths – KP-54, KP-14, KP-13 and KP-10, which are all able to stimulate their cognate receptor, KISS1 receptor (KISS1R). [57,58]

1.4.2 KISS1R

KISS1R, previously known as the orphan G-protein coupled receptor 54 (GPR54), is the natural target for kisspeptin. KISS1R consists of 398 amino acids and falls into the class A sub-family of GPCRs.[59,60] KISS1R is coupled to a $G\alpha_{q/11}$ protein which follows a G-protein dependent signalling cascade described in section 1.3.3. KISS1R and kisspeptin play an important role in the hypothalamic-pituitary-gonadal (HPG) axis, initiating puberty by releasing Gonadotrophin-releasing hormone (GnRH).[61] Since the first study in 1996, there have been a number of investigations in the role of kisspeptin/KISS1R in a number of different cancers, such as prostate cancer[62], bladder cancer[63], gestational trophoblastic disease[64], hepatocellular cancer[65], oesophageal carcinoma[66] and papillary thyroid cancer.[67] In the majority of these cancers, kisspeptin/KISS1R expression has been associated with anti-metastatic behaviour, however the role of kisspeptin and KISS1R in breast cancer is still unclear, as explained further in section 1.8.

1.5 Cancer

According to the World Health Organization (WHO), cancer is one of the leading causes of death worldwide, accounting for 1 in every 6 deaths.[68] It has been reported that by the year 2025, the burden caused by cancer will increase in low and middle-countries with new cases increasing by over 20 million each year. [69] Cancer can be defined as a group of heterogenous diseases characterised by uncontrolled cell proliferation, resulting in the formation of a tumour.[70] Treatment of cancer requires a multimodal approach, combining radiation therapy, chemotherapy, and surgery.[71]

Cancer cells develop when mutations occur in genes that are responsible for regulating cell proliferation and can be divided into proto-oncogenes and tumour suppressor genes. Proto-oncogenes encode transcription factors, growth factors and growth factor receptors, which are all responsible for initiating cell proliferation.[72] In contrast, tumour suppressor genes are important for the inhibition of cell proliferation and for the initiation of apoptosis. Activating mutations in proto-oncogenes and inactivating mutations in tumour suppressor genes remove the safeguards that prevent uncontrolled cell proliferation.[73]

Tumours can be classified according to their ability to invade surrounding tissue. Benign tumours are non-invasive and localised to one area of the body. They are less dangerous than malignant tumours but can cause complications if located near a vital organ or vessels.[74] Benign tumours are removed through surgery and have a low recurrence rate. Malignant tumours have the ability to invade surrounding tissues, enter the lymphatic or blood system and colonise secondary organs. Treatment options for malignant tumours usually include a combination of surgery and either radiation or chemotherapy. [74,75]

Cancer can affect the different tissues and organs of the body and are classified according to their origin. Figure 1.6 highlights the incidence and mortality rates of the 10 most prominent types of cancer worldwide, and specifically in South Africa (GLOBOCAN 2020).[76]

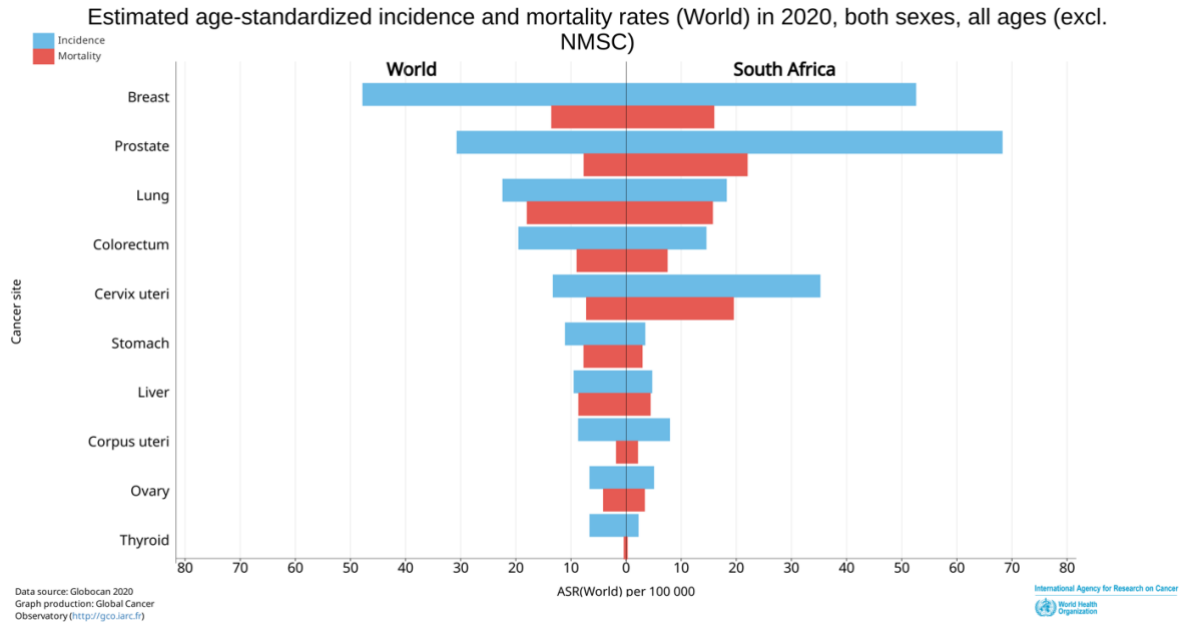

Figure 1.6: Diagram highlighting the estimated age-standardized incidence and mortality rate for different cancer origins worldwide and in South Africa in 2020.

Several cancer types such as prostate and cervical cancer occur at a higher incidence in South Africa, while mortality for many common cancers is also higher in South Africa when compared to global statistics. Image reproduced from Sung *et al* with permission from World Health Organisation.[76]

1.6 Breast cancer

In 2020, the estimated number of new cases of breast cancer in South Africa was 15 491, accounting for 14.3% of all new cancer cases (Figure 1.7).[76] Breast cancer is subdivided into five main sub-types (Table 1.2) based on the presence, absence or overexpression of the oestrogen receptor α (ERα), human epidermal growth factor 2 (HER2), and progesterone receptor (PR), as well the expression of Ki-67.[77]

Treatment of breast cancer can employ different approaches depending on the subtype and receptor composition. Chemotherapeutics target dividing cells, and are therefore used to treat all cancers. Breast cancer subtypes that have hormone receptors can be treated using hormone receptor targeting drugs such as tamoxifen, which is a selective oestrogen receptor modulator (SERD).[78] Due to the aggressiveness of triple negative breast cancers (TNBCs) and the lack of hormone receptors, identification of new treatment regimens for this type is imperative.

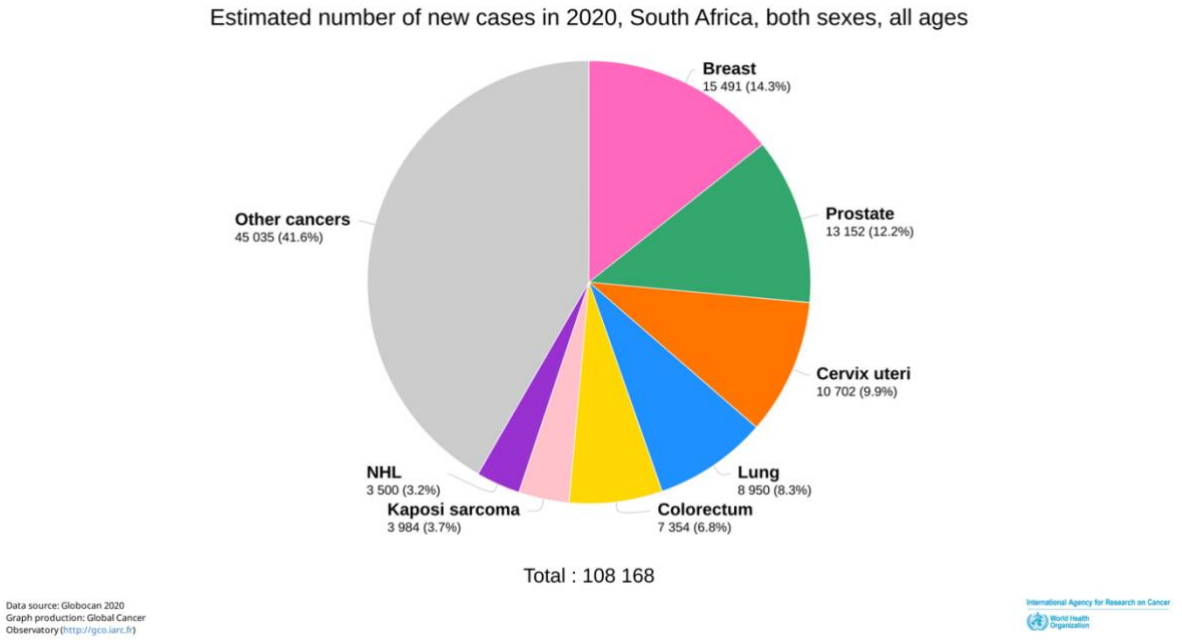

Figure 1.7: Estimated number of new cancer cases in South Africa in 2020.

Percentage of total cancer diagnoses in 2020 using GLOBOCON estimates generated by the International Agency for Research on Cancer. Image reproduced from Sung *et a*l with permission from World Health Organisation.[76]

Table 1.2: Subtypes of breast cancer classified according to their oestrogen receptor (ER), progesterone receptor (PR) , HER2 receptor and KI-67 profiles.[77]

Type of breast cancer	**Receptor composition**	**Characteristics**
Luminal A	ER + PR +/- HER2 – Ki-67 < 14%	Most common Accounts for 50-60% of all breast cancers Best prognosis
Luminal B	ER + PR+/- HER +/- Ki-67 > 14%	Accounts for 20% of all breast cancers Good prognosis Aggressive clinical behaviour[79]
HER2	ER- PR- HER2 overexpressed	Accounts for 15-20% of all breast cancers Poor prognosis Highly proliferative Treated with trastuzumab
Basal-like (Triple negative)	ER- PR- HER2 – KI-67	Accounts for 20% of all breast cancers Aggressive Younger age of onset Larger tumour size Higher proliferative index
Normal-like	ER- PR +/- HER2 – Low levels of KI-67	Accounts for 10 – 15% of all breast cancers Prognosis worse than luminal Can be treated with hormonal therapy

1.7 Metastasis

Stage four breast cancer is characterised by metastasis, the process by which cancer cells migrate from the primary tumour site in the breast to a secondary site. It has been shown that metastasis reduces the survival rate of patients when compared to patients with localised or regional cancer. The five year survival rate for localised breast cancer is 99% and 86% for regional breast cancer respectively, which drops to 27% when the cancer metastasises to a distant site.[80] The most common sites of breast cancer metastasis includes the bone, lungs, brain and liver.[81]

The cellular and molecular basis of metastasis was first described using the invasion-metastasis cascade proposed by Isaiah J. Fidler in 2003 and adapted by Scott Valastyan in 2011. It is proposed that metastasis occurs in six steps; local invasion, intravasation, survival in circulation, arrest in a distant organ site and extravasation, micrometastasis formation and metastatic colonisation, as highlighted by Figure 1.8.[82,83]

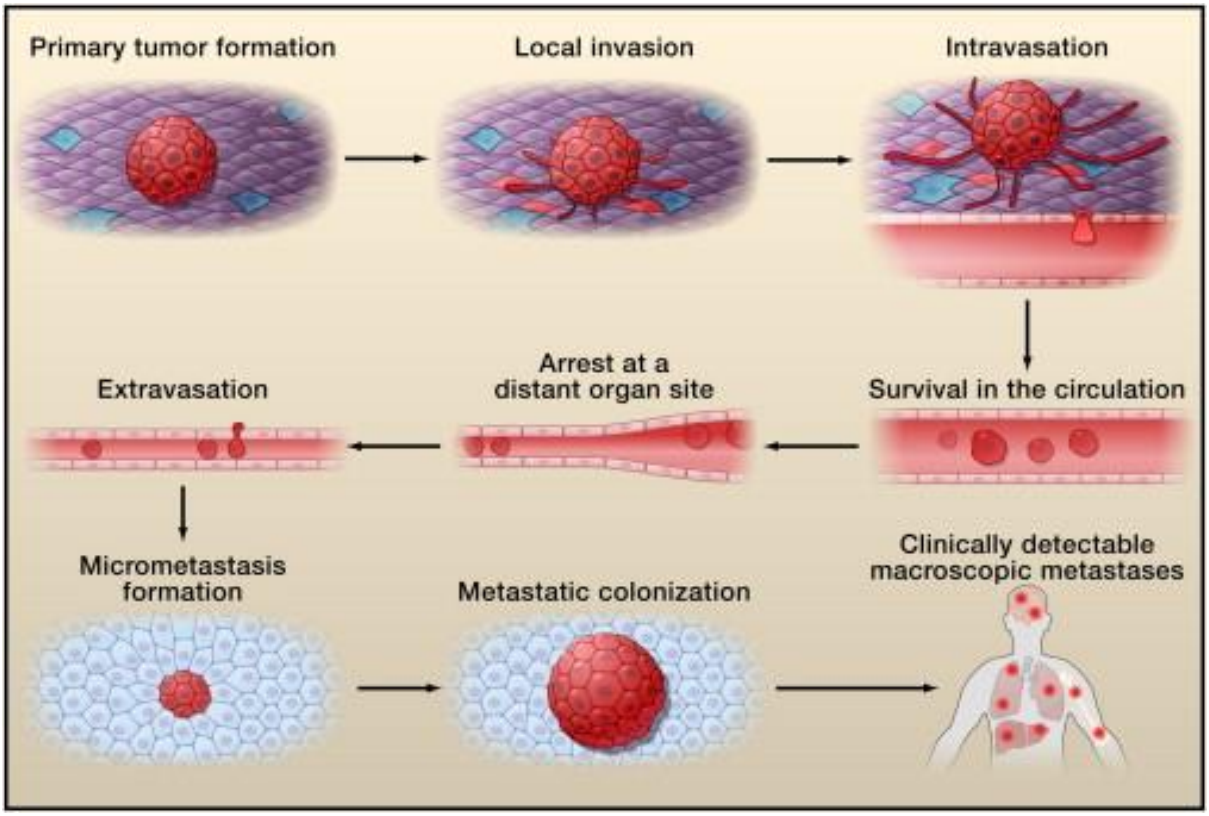

Figure 1.8: The invasion-metastasis cascade.

The steps that characterise metastasis include local invasion of the cancer cells into surrounding tissue, intravasation, survival in circulation, arrest at a distant organ site, extravasation, micrometastasis formation and metastatic colonization. Image reproduced from Valastyan *et al* with permission from Elsevier.[82]

There have been contrasting studies that have shown KISS1R to have both pro- and anti-metastatic behaviours in breast cancer.[75-80] Identifying the role of KISS1R in breast cancer could help in the identification of a novel drug target.

1.8 KISS1R and kisspeptin in breast cancer

A year after the KISS-1 gene was identified as a metastasis suppressor in melanoma cells, the same authors performed another study on breast cancer cells. They demonstrated that human breast cancer cells, MDA-MB-435 transfected with a KISS-1 gene demonstrated lower metastatic potential when compared to control cells.[84] It is important to note that this cell line has since been shown to be a melanoma cell line and not a breast cancer cell line.[85] Since then, multiple studies have gone on to provide evidence of the anti-metastatic behaviour of KISS1R. In a study performed by Kostadima *et al*, breast adenocarcinoma tissue was isolated from 272 stage two or three lymph-positive patients. Of all the samples, only 8 (2.9%) of these patients had detectable levels of *KISS1R*, which was suggested to have been downregulated to allow for metastasis.[86] Another compared *KISS1R* mRNA levels in primary breast cancer tissue and associated brain metastasis. *KISS1R* expression was significantly decreased in brain metastasis when compared to primary tissue, which coincides with the previous conclusion.[87]

In contrast, other studies have shown that KISS1R may play a pro-metastatic role.[79,80] Breast tissue samples were taken from patients and compared to healthy tissue samples. In breast cancer tissue, KISS1R was greatly expressed in the cytoplasm of cancer cells and other surrounding cells when compared to normal tissue. The same study also showed that *KISS1R* expression was significantly higher in node positive tumours compared to node negative tumours, and that tumours that had increased *KISS1R* expression were associated with poor prognosis and a higher tumour grade.[88] In a similar study, biopsies were taken from patients with TNBC and compared with healthy tissue samples. KISS1R mRNA and protein levels were significantly upregulated in TNBC samples when compared to healthy tissue.[89]

The articles that have sought to determine the role of KISS1R and kisspeptin in breast cancer metastasis have provided correlations but have failed to definitively show whether KISS1R/kisspeptin promotes or inhibits metastasis.[75-80] Due to the polarity of the research on KISS1R/kisspeptin and gene modulating technology available, this study aimed to develop a protocol to generate KISS1R breast cancer knockout (KO) cell lines with the aim to eventually determine the role of KISS1R/kisspeptin in breast cancer metastasis.

1.9 Aims and Objectives

The aim of this study was to modulate KISS1R expression in triple negative breast cancer cell line, MDA-MB-231, using either shRNA or CRISPR-Cas9 technology to determine the role of KISS1R in breast cancer metastasis.

The objectives for this project were:

1. To create a KISS1R knockdown MDA-MB-231 breast cancer cell line using an shRNA construct.
2. To develop a KISS1R knockout CRISPR-Cas9 protocol using HEK-293T cells.
3. To establish a KISS1R knockout MDA-MB-231 breast cancer cell line using CRISPR-Cas9 gene editing.

Chapter 2: Materials and methods

2.1 General materials

General materials and equipment that were used in all experiments and available commercially are highlighted in Table 2.1. Technique specific materials, reagents and equipment are described in the appropriate sections. All chemicals to make buffers were purchased from Sigma-Aldrich (Missouri, USA).

Table 2.1: General materials, reagents and equipment that were available commercially.

Item	**Catalogue number**	**Supplier**
2720 Thermal cycler	9002-18-0	Thermo Fisher Scientific, Massachusetts, USA
Eppendorf Centrifuge 5702	5702FG240241	Eppendorf, Hamburg, Germany
Falcon tube – 15 mL	188161	Greiner Bio-One, Kremsmünster, Austria
Falcon tube – 50 mL	227250	Greiner Bio-One, Kremsmünster, Austria
Orbital Shaker Incubator	LM-400D	Lasec, Randburg, RSA
Serological pipette – 5 mL	606180	Greiner Bio-One, Kremsmünster, Austria
Serological pipette – 10 mL	607107	Greiner Bio-One, Kremsmünster, Austria
Serological pipette – 25 mL	760107	Greiner Bio-One, Kremsmünster, Austria
Sigma 1-14K centrifuge	162104	Sigma Laborzentrifuge GmbH, Osterode, Germany

2.1.1 Plasmids

2.1.1.1 CRISPR-Cas9

The CRISPR-Cas9 plasmid, pSpCas9(BB)-2A-GFP PX458 was a gift from Feng Zhang laboratories (Addgene plasmid #48138;http://n2t.net/addgene:48138; RRID:Addgene_48138). This plasmid is 9299 base pairs (bp) in size and includes the Cas9 gene isolated from *Streptococcus pyogenes* (*S. progenes*) and a green fluorescent protein (GFP) gene that was used as the selectable marker (Figure 2.1). The plasmid contains a sgRNA scaffold in which the KISS1R sgRNA's were inserted.

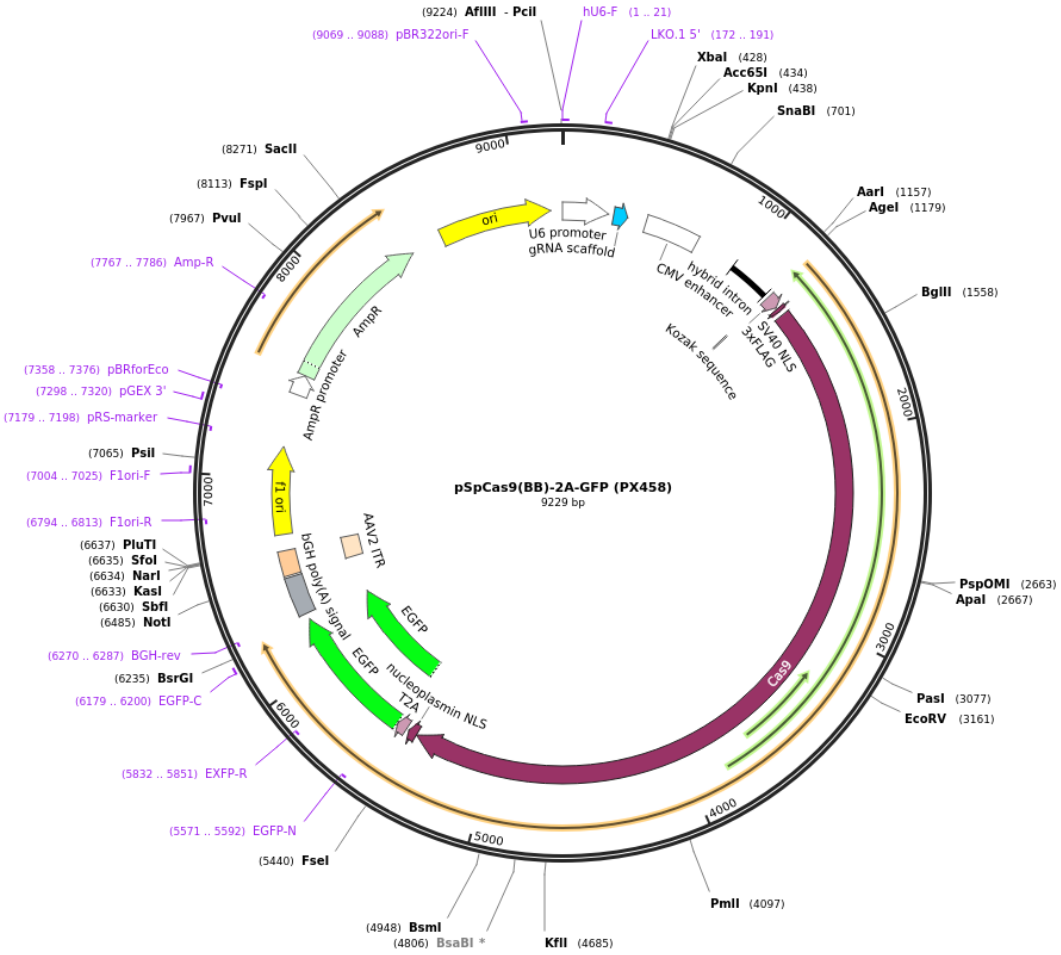

Figure 2.1: Diagram of the plasmid pSpCas9(BB)-2A-GFP PX45 used for this study.

The selected sgRNA's targeting KISS1R were inserted into the gRNA scaffold by digesting the plasmid with restriction enzyme *BbSI. (Addgene plasmid #48138; http://n2t.net/addgene: 48138; RRID:Addgene_48138).*

2.1.1.2 Short hairpin RNA

The KISS1R targeting shRNA (Table 2.2) and shRNA control plasmids (vector: pLKO.1 puro) had been generated in our laboratory prior to the initiation of this research study. The plasmids required to generate the shRNA lentiviral system were already available for use. (Table 2.3)

Table 2.2: KISS1R targeting shRNA.

shRNA	**Sequence (5'-3')**
Forward	CCGGGCGGCTATTCTTCTGTTATTACTCGAGTAATAACAGAAGAATAGCCGCTTTTTG
Reverse	AATTCAAAAAGCGGCTATTCTTCTGTTATTACTCGAGTAATAACAGAAGAATAGCCGC

Table 2.3: Plasmids used to generate the shRNA-lentiviral system.

Name	Plasmid number on Addgene	Purpose
pCMV-dR8.2 dvpr	8455	Lentiviral packaging
pCMV-VSV-G	8454	Envelope protein
pLKO.1 puro	8453	Lentiviral backbone for cloning and expressing shRNA sequences

2.1.2 Single guide RNAs

CRISPOR (http://crispor.tefor.net/) is an online selection tool first created by Haeussler and Concordet in 2016, that uses an algorithm to identify targets in genes of interest, design sgRNA's, identify off target sites, and design primers.[90] CRISPOR was used to identify five sgRNA's targeting KISS1R (Table 2.4). sgRNA sequences should be between 17 and 24 nucleotides long and have a GC content between 40-80%. Due to the unpredictability of sgRNA's it is suggested to design and test at least five different sgRNA's.

Table 2.4: The sgRNA designed to target the KISS1R ORF.

sgRNA	Sequence (5'-3')
1	AAGTTGGTCACGGTCCGCA
2	TCCGGACCCAACGCGTCCT
3	TCACGGTCCGCATCGGCTTG
4	TGTGGCGCCAACGCCTCGGA
5	CCCCCAGGACGCGTTGGGTC

2.1.3 Primer design

Primer pairs that amplify β-Actin (ACTB) open reading frame (ORF) (1) (Accession number: NM_001101.5) and KISS1R ORF (2) (Accession number: NM_032551.5) regions from cDNA were already available for use in the Centre for Neuroendocrinology's laboratory. CRISPOR was used to design a primer pair (3) that amplified a 798 bp region in the KISS1R gene in which our sgRNA's were targeting for the T7 endonuclease assay. A vector screening primer pair (4) that binds upstream of the sgRNA scaffold and at the *BBSI* restriction site was designed by Addgene, and synthesized by Integrated DNA Technologies (Iowa, USA). (Table 2.5) These primers were synthesized by Inqaba Biotechnical Industries (Pretoria, RSA).

Table 2.5: Information on PCR primers used in this research study.

	Name	Sequence (5' – 3')	Melting temp	Annealing temp	Size (bp)
1	RT-PCR: Human ACTB set 1 forward primer Human ACTB set 1 reverse primer	CAGAGCCTCGCCTTTGC CTCGTCGCCCACATAGGA	56.8°C 56.6°C	52.0°C	225
2	RT-PCR: Human KISS1R set 2 forward primer Human KISS1R set 1 reverse primer	CAACTTCTACATCGCCAACC AGCAGGTTGTACAGTGCGA	53.7°C 56.7°C	55.0°C	399
3	T7 Endonuclease assay: KISS1R forward primer KISS1R reverse primer	TTGCCGCTGGGTGAATAGAG AGGTTTCCATGTGCCACA CT	53.83°C 51.78°C	49°C	798
4	Vector screening: Forward primer Reverse primer	GAGGGCCTATTTCCCATGATTCC TCTTCTCGAAGACCCGGTG	59°C 58°C	53°C	264

2.2 Molecular biology techniques

2.2.1 Materials

Materials, equipment and reagents that were used for molecular biology techniques that were available commercially are listed in Table 2.6, and reagents made in-house are listed in Table 2.7.

Table 2.6: Materials, equipment and reagents used for molecular techniques that are available commercially.

Item	Catalogue number	Supplier
ABI3500xl Genetic Analyser instrument	4406016	Thermo Fisher Scientific, Massachusetts, USA
Agarose and Polymerase Chain Reaction (PCR) clean-up kit	740609	Macherey-Nagel, Duren, Germany
Alkaline Phosphatase – Calf Intestinal	M0525L	New England Biolabs, Massachusetts, USA
BigDyeTM Terminator V3.1 cycle sequencing kit	4337458	Thermo Fisher Scientific, Massachusetts, USA
BbSI	R0539S	New England Biolabs, Massachusetts, USA

Chemidoc MP imaging system	73BR02464	BioRad Laboratories, California, USA
Deoxynucleotide (dNTP) mix	N0447S	New England Biolabs, Massachusetts, USA
DNA ladder – 1 kb plus	10787018	Thermo Fisher Scientific, Massachusetts, USA
EDTA	17892	Thermo Fisher Scientific, Massachusetts, USA
Ethanol – molecular grade	E7023	Sigma-Aldrich, Missouri, USA
Gel loading dye, 6x, purple	B7024S	New England Biolabs, Massachusetts, USA
GelRed® Nucleic Acid Gel Stain	41003	Biotium, California, USA
GeneAmp® PCR system 9700	4339386	Thermo Fischer Scientific, Massachusetts, USA
LunaScript® RT SuperMix kit	E3025S	New England Biolabs, Massachusetts, USA
Mini-Sub Cell GT Cell gel tank	1704406	BioRad Laboratories, California, USA
Macherey-Nagel™ Nucleospin™ DNA RapidLyse mini-kit	740100	Macherey-Nagel, Duren, Germany
Macherey-Nagel™ NucleoSpin™ Plasmid EasyPure kit	740727	Macherey-Nagel, Duren, Germany
NanoDrop™ 1000 spectrophotometer	ND-1000	Thermo Fisher Scientific, Massachusetts, USA
NEBuffer 2	B7002S	New England Biolabs, Massachusetts, USA
OneTaq® DNA Polymerase	M0480S	New England Biolabs, Massachusetts, USA
OneTaq® GC reaction buffer	B9023	New England Biolabs, Massachusetts, USA
RNeasy™ Mini kit	74004	Qiagen, Hilden, Germany.
Taq 2x MasterMix	M0270L	New England Biolabs, Massachusetts, USA
T4 DNA Ligase	M0202	New England Biolabs, Massachusetts, USA
T4 DNA Ligase reaction buffer	B0202S	New England Biolabs, Massachusetts, USA

Table 2.7: Reagents required for molecular techniques that were made in house.

Item	Components
Agar plates	• 1% (w/v) tryptone • 0.5% (w/v) yeast extract • 170 mM NaCl • 1.5% (w/v) agar • 100 µg/ml ampicillin
Luria-Bertani (LB) broth	• 1% (w/v) tryptone • 0.5% (w/v) yeast extract • 170 mM NaCl
Tris-Acetic acid-EDTA, 1x	• 40 mM Tris base • 49 mM acetic acid • 1 mM EDTA

2.2.2 Methods

2.2.2.1 Cloning strategy

2.2.2.1.1 Restriction digest

The cloning strategy developed and optimized by Zhang laboratories (https://www.addgene.org/crispr/reference/#protocols) was followed to insert each sgRNA into the plasmid. Briefly, 1.4 µg of the CRISPR-Cas9 plasmid was combined with 10 U of the restriction enzyme *BbsI*, alkaline phosphatase and NEBuffer™ 2.1 and incubated at 37˚C for 30 min before being resolved using agarose gel electrophoresis.

2.2.2.1.2 Agarose gel electrophoresis

A 1% (w/v) agarose gel was made by combining and heating 1x TAE buffer and agarose in a microwave, to melt the agarose. Once the beaker was cool to touch, GelRed® Nucleic Acid Gel Stain was added in a dilution of $\frac{1}{30\ 000}$. Purple gel loading dye was added to DNA samples to achieve a final concentration of 1x. Agarose gels were electrophoresed at 120V for 30 min in a Mini-Sub Cell GT Cell gel tank and a Chemidoc MP imaging system was used to visualise DNA. The accurate product size was determined using an appropriate DNA ladder loaded in the first lane of each agarose gel.

2.2.2.1.3 DNA purification

The plasmid DNA fragments were excised from the agarose gel and purified using a Agarose and Polymerase Chain Reaction (PCR) clean-up kit. Briefly, excised agarose gel containing the digested plasmid was melted in the provided buffer at 50°C, and the DNA captured on a Nucleospin™ Gel and PCR Clean-up column. After the specified wash steps, 30 µL of the provided elution buffer was added to the column and incubated at room temperature for 1 min. After incubation, the column was centrifuged at 6 000 x *g* for 1 min to elute the DNA before DNA quantification on a Nanodrop1000™ spectrophotometer.

2.2.2.1.4 Ligation

Prior to assembling the ligation reactions, the sense and antisense sgRNA's (1:1 ratio) were annealed in T4 DNA ligase buffer by heating to 95°C and then gradually cooling the reaction to 25°C. Purified plasmid was then ligated with each sgRNA by combining the components highlighted in Table 2.8. A ligation control was included. Combined reactions were incubated at room temperature for 10 min before they were transformed in XL10-Gold *E. coli*.

Table 2.8: Different ligation reactions.

Sample	**Composition**
Ligation control	• 50 ng of plasmid DNA • 1 U of ligase • 2 µL of ligase buffer • To 20 µL using RNAse-free water
sgRNA recombinant mix 1-5	• 50 ng of plasmid DNA • 1 µL of annealed sgRNA 1/2/3/4/5 (1:200) • 1 U of ligase • 2 µL of ligase buffer • To 20 µL using RNAse-free water

2.2.2.2 Transformation

Ligation reactions were transformed by combining 40 µL XL10-Gold *E. coli* competent cells and 10 µL of each ligation reaction in a 0.5 mL tube. A transformation control (containing water) was included. Reactions were incubated on ice for 30 min before heat-shock at 42°C for 90 sec. Reactions were immediately placed on ice for 2 min and 0.5 ml of LB broth was added prior to incubating for 1 h at 37°C in a shaking incubator. The tubes were centrifuged at 3000 x *g* for 3 min, after which, 0.4 ml of the supernatant was removed. Each pellet was resuspended,

and transferred to individual agar plates made with ampicillin and spread aseptically. Agar plates were incubated at 37ºC overnight.

2.2.2.3 Plasmid Purification

The NucleoSpin™ Plasmid EasyPure kit was used to isolate plasmid DNA from bacterial cells as per the manufacturer's protocol. A NanoDrop1000™ spectrophotometer was used to determine the plasmid DNA concentrations. Isolated plasmid DNA samples were deemed pure if their 260/280 ratio was approximately 1.8.

2.2.2.4 Reverse transcriptase-Polymerase Chain Reaction

Reverse transcriptase-PCR (RT-PCR) was used to assess *KISS1R* mRNA levels in cell lines transfected and transduced with the KISS1R targeting shRNA construct. RNA was extracted from the HEK-293T and MDA-MB-231 cell lines using the RNeasy™ Mini kit, as per the supplier's protocol. After extraction, 1 µg RNA was used to synthesize complementary DNA (cDNA), and the remaining RNA stored at -80°C. cDNA was synthesized using the LunaScript® RT SuperMix kit per the supplier's protocol.

PCR reactions were prepared as indicated by Table 2.9 and the cycling conditions highlighted in Table 2.10 were used. A negative control (without cDNA) was included in the analysis.

Table 2.9: The components required for the PCR to amplify the KISS1R target sequence from isolated cDNA.

Component	**For 1 reaction (µL)**
Taq x2 Mastermix	12.5
Forward primer (10 µM)	0.5
Reverse primer (10 µM)	0.5
DMSO (3%)	0.75
Nuclease-free water	8.75
cDNA	2
Final volume	25

Table 2.10: The PCR conditions required for the above reaction.

Temperature	Time	Cycles
95℃	30 sec	
95℃	30 sec	30
*52℃	30 sec	
68℃	30 sec	
68℃	5 min	
4℃	∞	hold

*T_a = Tm-5

2.2.2.5 T7 endonuclease assay

The T7 endonuclease assay was used to determine the editing efficiency achieved with each sgRNA in an unsorted population. This was done to decide which two sgRNA's would be used to generate the KO cell lines. This assay was also used to identify single cell clones which were positive for INDEL mutations.

This assay follows the workflow as depicted by Figure 2.2. Briefly, genomic DNA was isolated from transfected cell populations using a Macherey-Nagel™ Nucleospin™ DNA RapidLyse mini-kit as per the manufacturer's instructions. Next, a PCR was performed to amplify a 798 bp region of the KISS1R gene where the sgRNA's are targeted. PCR reactions are detailed in Table 2.11 with a negative control containing genomic DNA from cells transfected with the empty plasmid vector, and a control containing nuclease-free water included for each PCR. PCR reactions were run using the touch-down conditions highlighted by Table 2.12.

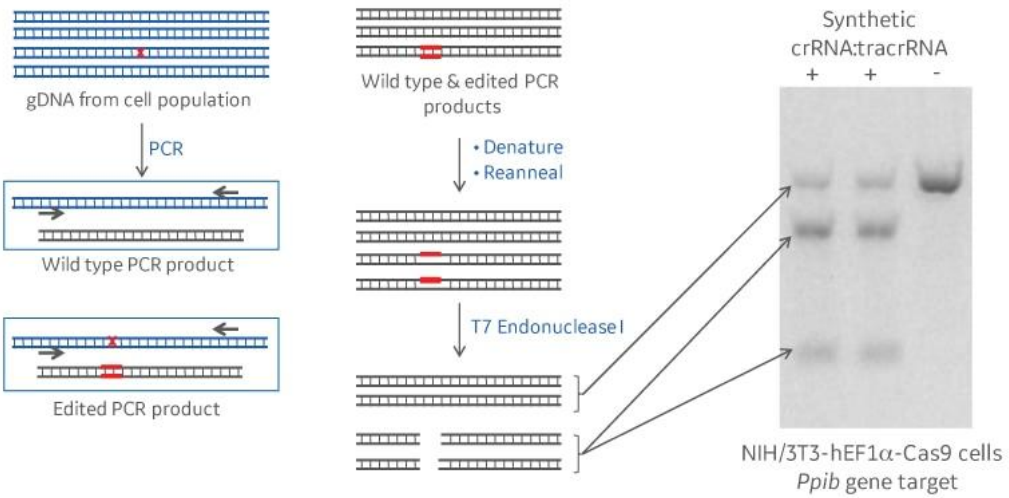

Figure 2.2: T7 endonuclease assay work-flow.

A PCR is performed on isolated genomic DNA to amplify the targeted region. PCR products are denatured, reannealed and digested with the T7 endonuclease I enzyme. Digested products are resolved on a 1% agarose gel. Image reproduced from Kerschgens with permission from Horizon Discovery Ltd.[91]

Table 2.11: The components required for the OneTaq® PCR reaction.

Component	**1 reaction (µL)**
5x OneTaq® GC reaction buffer	10
10 nM dNTP's	1
10 µM forward primer	1
10 µM reverse primer	1
OneTaq® DNA Polymerase	0.25
DMSO	1.5

Table 2.12: The conditions required for the OneTaq® PCR reaction.

Temperature (ºC)	**Duration**	**Cycles**
95	3 min	
95	30 sec	3
52	30 sec	
72	2 min	
95	30 sec	30
49	30 sec	
72	2 min	
72	7 min	

To ensure successful amplification of the 800 bp region, 10 µL of the PCR reactions were combined with 6x loading dye to a final concentration of 1x, and agarose gel electrophoresis was performed as described in section 2.2.2.1.2. Gels were visualised using a ChemiDoc MP imaging system. The remaining sample was purified using the Agarose and Polymerase Chain Reaction clean-up kit as per the manufacturers protocol.

Purified PCR products were denatured and reannealed by combining components according to Table 2.13. Reactions were placed into a GeneAmp® PCR system 9700 and cycling conditions were conducted as described in Table 2.14.

Table 2.13: Components combined to denature and reanneal PCR products.

Components	**Amount**
10x NEBuffer™2	2 µL
DNA	200 ng
Nuclease-free water	to 19 µL

Table 2.14: PCR conditions used to denature and reanneal PCR products for the T7 endonuclease assay.

Temperature	**Ramp rate**	**Time**
95ºC		5 min
95-85ºC	-2ºC/second	
85-25ºC	-0.1ºC/second	
4ºC		∞

After reannealing, 1 µL of T7 endonuclease I was added to each sample and incubated at 37ºC for 15 min before the addition of 0.01M Ethylenediaminetetraacetic acid (EDTA). Agarose gel electrophoresis was performed using the method described in section 2.2.2.1.2.

The intensity of each band was determined using ImageLab software 6.1 developed and distributed by Bio-Rad Laboratories, and the background subtracted from each value. The percentage of gene modification was determined using the formula below.

$$\% \text{ Gene modification} = 100 \times (1-(1-\text{fraction cleaved})^{1/2})$$

2.2.2.6 Sanger Sequencing

Sanger sequencing was performed using the BigDye™ Terminator V3.1 cycle sequencing kit as per the supplier's protocol to confirm the insertion of the sgRNA's into the vector, as well as provide data for the Inference of CRISPR edits (ICE) analysis on single cell clones (section 2.3.2.8) in which INDEL mutations were detected. Briefly, the components listed in Table 2.15 were combined in 0.2 mL PCR tubes. PCR tubes were placed into a 2720 Thermal cycler and a PCR was conducted according to the cycling conditions outlined in Table 2.16.

Table 2.15: Components required for Sanger Sequencing reactions.

Components	**Amount**
1x BigDye	1 µL
Sequencing buffer – 5x	2 µL
Sequencing primer – 3.2 µM	1 µL
DNA	100 ng
Nuclease-free water	To final volume of 10 µL

Table 2.16: PCR conditions for Sanger sequencing reactions.

Steps	**Temperature**	**Time**
Initial denaturation	96ºC	1 min
25 cycles	96ºC	10 sec
	50ºC	5 sec
	60ºC	2 min
	4ºC	∞

DNA was precipitated by adding 1.5 µL of 3 M sodium acetate (pH 4.6), 31.5 µL of molecular grade ethanol and 7.25 µL of ultrapure water. Reactions were incubated on ice for 15 min, and then centrifuged at 16 000 x *g* for 20 min at 4ºC in a Sigma 1-14K centrifuge. The supernatant was aspirated, and the DNA pellets washed twice with 70% (v/v) molecular grade ethanol, and centrifuged at 16 000 x *g* for 5 min at 4ºC. The supernatant was aspirated and the DNA pellets dried in an oven at 37ºC for at least 30 min. DNA was sequenced on a ABI3500xl Genetic Analyser instrument by the DNA Sanger Sequencing Facility found at the University of Pretoria (Pretoria, South Africa). Samples with a quality score of more than 25 were analysed using CLC Bio Workbench.

2.3 Cell culture

2.3.1 Materials

HEK-293T (CRL-1573) and MDA-MB-231 (HTB-26) (Table 2.17) cell lines were originally obtained from the American Type Culture Collection (Virginia, USA). Core stocks were available for use at the Centre for Neuroendocrinology's laboratory. All cell culture techniques were conducted using standard aseptic techniques. General cell culture equipment and consumables are described in Table 2.18 and recipes for in house reagents are listed in Table 2.19.

Table 2.17: The main cell types used for this study.

Cell line	**Media type**	**Doubling-time**	**Trypsinization time**	**Note**	**Passage dilution**
HEK-293T	DMEM	24 h	3 min	Supplemented with 10% FCS	1:4
MDA-MB-231	DMEM	24 h	5 min	Supplemented with 10% FCS	1:4

Table 2.18: Equipment, materials and reagents required for cell culture that are available commercially.

Item	**Catalogue number**	**Supplier**
Airstream® Gen 3 Vertical Laminar Flow Cabinet	LVS-4AG-S	Life Sciences group, Bedfordshire,UK
BD FACSAria™ Fusion Flow cytometer	23-14994-01	BD Biosciences, New Jersey, USA
CytoFLEX SRT Benchtop Cell Sorter	01-1234	Beckman Coulter, California, USA
Cell culture flasks, 50 mL, 25 cm^2 (T25)	690940	Greiner Bio-One, Kremsmünster, Austria
Cell culture flasks, 250 mL, 75 cm^2 (T75)	658940	Greiner Bio-One, Kremsmünster, Austria
Cell scraper, 28 cm long, blue, sterile,	541070	Greiner Bio-One, Kremsmünster, Austria
Corning® Matrigel® matrix	356235	Corning Incorporated, New York, USA
Countess™ II Automated Cell Counter	C19228	Thermo Fisher Scientific, Massachusetts, USA
Countess™ Cell Counting Chamber Slide	AMQAX1000	Thermo Fisher Scientific, Massachusetts, USA
Cryo.S™ cryovials	126280	Greiner Bio-One, Kremsmünster, Austria
CytoFLEX	C71888	Beckman Coulter, California, USA
Dimethyl Sulfoxide (DMSO)	D8418-1L	Sigma-Aldrich, Missouri, USA
Eppendorf Centrifuge 5702	5702FG240241	Eppendorf, Hamburg, Germany
Foetal calf serum/ Foetal bovine serum (FCS/FBS)	10270106	Thermo Fisher Scientific, Massachusetts, USA
Gibco Dulbecco's Modified Eagle Medium (DMEM), high glucose, GltaMAX™ supplement	10566016	Thermo Fisher Scientific, Massachusetts, USA
Gene Pulser® Electroporation system with capacitance extender	165-2660	Bio-Rad Laboratories, California, USA
Gene Pulser®/MicroPulser™ Electroporation Cuvettes 0.2 cm gap	1652086	Bio-Rad Laboratories, California, USA
Glass pasteur pipette	GLAS2P20M230	Lasec, Randburg, RSA

Isopropyl alcohol	I9516 – 1L	Sigma-Aldrich, Missouri, USA
Minisart® NML Plus Syringe Filter 17829---------K, GF + 0.45 µm Surfactant-free Cellulose Acetate	17829	Sartorius, Göttingen, Germany.
Nalgene® Mr. Frosty Cryo 1°C Freezing Container	5100-0001	Thermo Fisher Scientific, Massachusetts, USA
Trypan blue stain 0.4%	T10282	Thermo Fisher Scientific, Massachusetts, USA
Trypsin-EDTA (0.25%)	25200072	Thermo Fisher Scientific, Massachusetts, USA
XtremeGene HP DNA transfection reagent	6366236001	Sigma Aldrich, Missouri, USA
Zeiss Primo Vert.A1 Inverted microscope	491237-0014-000.	ZEISS, Jena, Germany

Table 2.19: Recipes for materials required for cell culture that were made in house.

Item	**Components**
Cryopreservation media	• 10% DMSO • 40% FCS/FBS
Growth Media	• 500 mL DMEM • 50 mL FCS/FBS
Mannitol buffered phosphate – electroporation buffer	• 5 mM Potassium Chloride (KCl) • 15 mM Magnesium Chloride ($MgCl_2$) • 120 mM Disodium Hydrogen Phosphate (Na_2HPO_4) • 50 mM D-Mannitol • pH adjusted to 7.2 • Filter sterilised under aseptic conditions using a 0.2 µm filter
1x Phosphate Buffered Saline (PBS)	• 137 mM Sodium Chloride (NaCl) • 2.7 mM Potassium Chloride (KCl) • 10 mM Disodium Hydrogen Phosphate (Na_2HPO_4) • 1.8 mM Potassium dihydrogen phosphate (KH_2PO_4) • pH adjusted to 7.4

2.3.2 Methods

2.3.2.1 Raising cells

Core stocks of cell lines were stored in liquid nitrogen in Cryo.S™ cryovials until they were required. Prior to experimentation, a vial of each cell type (containing approximately 1 mL of cell suspension) was removed from liquid nitrogen storage. The cell suspensions were rapidly thawed and immediately added to 5 mL of the appropriate pre-warmed growth media (Table 2.17) in a 15 mL polypropylene tube. Cell suspensions were centrifuged at 800 x *g* for 3 min using a 5702 Eppendorf Centrifuge, followed by removal of the supernatants. Cell pellets were suspended in 5 mL of growth media and transferred to labelled T25 flasks before incubating overnight at 37°C, 5% CO_2, with 90% relative humidity (RH).

2.3.2.2 Passaging

Cell lines were grown to approximately 80% confluency before passaging. Media was aspirated and a single wash-step using 1x Phosphate buffered saline (PBS) was conducted. Trypsin-EDTA was added to the cells to detach them followed by incubation for the appropriate amount of time (Table 2.17). After incubation, growth media was added to the plate or flask to inactivate trypsin-EDTA activity. The cell suspension was transferred to a new 15 mL polypropylene tube and centrifuged at 800 x *g* for 3 min. Supernatant was aspirated, and the cell pellet was suspended in growth media. A portion of this cell suspension was added back to a plate or flask already containing the appropriate amount of growth media. The cells were then incubated at 37°C, 5% CO_2, with 90% RH.

2.3.2.3 Freezing of cells

To ensure that core stocks of these cell lines were maintained, cells were cryopreserved in regular intervals. After passaging, the concentration of live cells was determined by adding 10 µL of the cell suspension and 10 µL of 0.4% trypan blue to a 0.5 mL microcentrifuge tube. To each chamber of a Countess™ Cell Counting Chamber Slide, 10 µL of the trypan blue stained cell suspension was added. The slide was inserted into the Countess™ II automated cell counter and the cell count determined. To each cryovial, $1x10^6$ live cells combined with cryopreservation media in a 1:1 ratio was added. The cryovials were stored in a

Mr. Frosty™ containing isopropyl alcohol in a -80°C freezer overnight. The following day, cryovials were moved to liquid nitrogen for long-term storage.

2.3.2.4 Seeding

Cells were seeded at different concentrations for different assays as stipulated in Table 2.20. Prior to seeding HEK-293T cells, plates were coated with Corning® Matrigel® matrix for at least 45 min. The concentration of cell suspensions were determined as described in section 2.3.2.3.

Table 2.20: Cell seeding densities for various experiments.

Experiment	**Cell line**	**Seeding density (cells/well)**	**Plate size**
Lentivirus production	HEK-293T	5 x10^5	6 well plate
Lentivirus infection	HEK-293T	3 x10^5	6 well plate
CRISPR-Cas9 construct transfection	HEK-293T	3 x10^5	6 well plate
	MDA-MB-231	3 x10^5	6 well plate

2.3.2.5 Lipofection

Cells were transfected using XtremeGene™ HP DNA transfection reagent, as per the manufacturer's protocol. Briefly, a transfection mix containing DNA in a ratio of either 1 µg to 2 µL or 1 µg to 3 µL of the transfection reagent, diluted in serum-free media (SFM) was made. Transfection mix was vortexed and left to incubate for 15 min at room temperature before being added to each well. Plates were incubated overnight at 37°C, 5% CO_2, with 90% RH.

2.3.2.6 Lentiviral production

To generate the KISS1R shRNA and control shRNA containing lentivirus, 5 x 10^5 HEK-293T cells were added to each well in a 6 well plate. The following day, cells were transfected using polyethylenimine (PEI) with the shRNA constructs (Table 2.21) in the ratio's specified in Table 2.21. The transfection mix was incubated for 20 min at room temperature and added to the cells. The following morning, media was replaced with 2 mL of DMEM and left to incubate for 24 h. Media containing lentivirus was collected from each well and placed in a 15 mL tube, at 4°C, approximately 36 h post-transfection. Fresh media was added to each well and incubated overnight before a final batch of lentivirus was collected and added to

the first batch. Lentivirus media was filtered using a 0.45 Minisart© filter and was either used the same day or stored at -80°C until required.

Table 2.21: Components used to create shRNA containing lentivirus.

Construct	Amount added
pCMV-dR8.2 dvpr	1100 ng
pCMV-VSV-G	570 ng
pLKO.1 puro (KISS1R-targeting or control shRNA)	2300 ng
PEI	12.5 µL

2.3.2.7 Electroporation

MDA-MB-231 cells were harvested using the protocol stipulated in section 2.2.2.2, and live cell count was determined (section 2.3.2.3). The required volume of cell suspension was added to a 1.5 mL tube to ensure the presence of 2 x 10^6 live cells. The cells were centrifuged at 800 x *g* for 3 min, the supernatant aspirated and a single wash-step using 1x PBS was performed. The PBS was aspirated, and the cell pellet suspended in 250 µL of mannitol-buffered phosphate electroporation buffer containing 10 µg of the CRISPR-Cas9 sgRNA constructs. Electroporation was performed using Bio-Rad's Gene Pulser® II with the capacitance extender using Gene Pulser® electroporation cuvettes with a 0.2 cm gap. After electroporation, the cells were added to a 6 well plate already containing pre-warmed media and left to attach overnight.

2.3.2.8 Single cell isolation

2.3.2.8.1 Dilutions

To isolate single HEK-293T cells, the concentration of the transfected cells was determined as per section 2.3.2.3. The cell suspension was then diluted to a concentration of 20 cells/mL. To a Matrigel-coated 96 well plate, 200 µL of this 20 cells/mL cell suspension was added, with the aim of isolating GFP-positive single cells for expansion of single cell clones. Theoretically, 4 cells will be plated per well, however, in practice while a few wells will contain 4 cells, others will contain less.

2.3.2.8.2 Cytoflex SRT cell sorter

MDA-MB-231 cells were harvested 48 h post-electroporation and taken to a private laboratory to be sorted. A negative control, MDA-MB-231 cells electroporated in the absence of plasmid DNA was first run to locate the population of interest and determine the level of auto-fluorescence. GFP-positive cells were bulk sorted into media containing penicillin-streptomycin antibiotic, as the sorter was not sterile. Once the samples had been sorted, cells were diluted to a concentration of 20 cells/mL and 200 µL added to each well of a 96 well plate.

2.3.2.8.3 FACSAria™ Fusion cell sorter

MDA-MB-231 cells were harvested 48 h post-electroporation, and one GFP-positive cell was added to each well in a 96 well plate using a FACSAria™ Fusion cell sorter. A negative control, MDA-MB-231 cells electroporated in the absence of plasmid DNA was first run to locate the population of interest and determine the level of auto-fluorescence.

2.4 Calcium signalling assay

Due to the absence of specific antibody for KISS1R, we were unable to confirm knockdown or knockout of KISS1R at a protein level. To overcome this limitation, downstream signalling in response to KP-10 stimulation was assessed using a calcium signalling assay optimised in our laboratory.

2.4.1 Materials

The materials required for the calcium signalling assay that are available commercially are listed in Table 2.22, and the reagents prepared in-house are listed in Table 2.23.

Table 2.22: Materials required for the calcium signalling assay that are available commercially.

Item	**Catalogue number**	**Supplier**
µ-slide Ibidi plate, 8-well	80826	Ibidi, Grafelfing, Germany
Bovine serum albumin (BSA)	0332-500G	VWR chemicals, Pennsylvania, USA
Fluo-3-AM – 1 mM stock dissolved in 100% DMSO	F1241	Thermo Fisher Scientific, Massachusetts, USA
Ionomycin – 5 mM stock dissolved in 100% DMSO	124222	Thermo Fisher Scientific, Massachusetts, USA
Kisspeptin-10 (KP-10) – 1 mM stock dissolved in 100% DMSO	205403	GL Biochem (Shanghai) Ltd, Shanghai, China.
Pluronic® F-127	P2443	Sigma-Aldrich, Missouri, USA
Probenecid	P8761	Sigma-Aldrich, Missouri, USA

Table 2.23: Materials required for the calcium signalling assay that were prepared in-house.

Reagent	**Composition**
Calcium chloride – 0.9 M	• 10 g of Calcium Chloride was dissolved in 100 mL of distilled water
Fluo-3-AM loading solution	• 2.5 µM Fluo-3-AM in HBSS-BSA-Probenecid buffer containing Pluronic® F-127
Hank's balanced salt solution (HBSS), 10 x	• 5.4 mM Potassium chloride (KCl) • 0.5 mM Magnesium chloride hexahydrate (MgCl2-6H2O) • 0.4 mM magnesium sulphate heptahydrate (MgSO4-7H2O) • 0.4 mM potassium dihydrogen phosphate (KH2PO4) • 0.34 mM disodium hydrogen phosphate heptahydrate (Na2HPO4-7H2O) in 1000 ml of distilled water added and stored at 4ºC
HBSS, 1x	• For 1000 ml, 100 ml of 10× HBSS was mixed with 800 ml of distilled water. To this, 1.3 mM of anhydrous CaCl2, 5.5 mM of d-glucose and 4.2 mM of NaHCO3 was added. The volume was adjusted to 1000 mL with distilled water, the pH adjusted to 7.4 and stored at 4ºC
HBSS-BSA-Probenecid	• 45 mL of 1x HBSS • 1 mg/mL of BSA • 2.5 mM of Probenecid
Pluronic F127 – 20%	• 2 g of Pluronic F-127 was added to 10 mL of 100% DMSO • Solubilised by heating at 40ºC for 20 min.
Probenecid - 1M	• 7.135 g of probenecid powder was added to 25 mL of 1 M NaOH • Heated for 30 min on an magnetic stirrer. Stored at -20ºC

2.4.2 Methods

The calcium signalling assay was used to compare the release of calcium into the cytosol, after stimulation with KP-10, between the MDA-MB-231 shRNA control and MDA-MB-231 KISS1R shRNA cell lines. This was achieved using the calcium indicator dye, Fluo-3-AM. This assay was performed using a Zeiss LSM800 laser scanning confocal microscope with temperature control set to the Fluo-3 channel, with an excitation and emission wavelength of 506 nm and 527 nm respectively. A 20x objective with a numerical aperture of 0.5 was used and the confocal scanning system set to a fast-scanning mode. An image was created from 512 × 512 pixels every 1.5 sec with 401 frames, with the pinhole set to 2.27 AU. Prior to experimentation, the microscope was turned on at least 30 min before and the temperature of the microscope's heating chamber set to 37ºC.

Both cell lines were seeded in 200 µL of growth media in an 8 well Ibidi microslide plate, and incubated overnight at 37 ºC, 5% CO_2 and 95% RH. The following day, 180 µL of the growth media was replaced with the Fluo-3-AM loading solution and incubated in the dark at 37ºC in a humidified incubator under standard conditions. After the incubation period, the loading dye was removed and the wells were washed three times with HBSS-BSA-probenecid buffer. After the wash steps, 180 µL of HBSS-BSA-probenecid buffer was added and the cells incubated for 30 min under standard cell culture conditions. After the incubation period, the microslide was put into the chamber of the microscope, with its lid removed. The video was started prior to the addition of KP-10 in order for a baseline fluorescence measurement to be determined during analysis. After 75 sec, 100 nM of KP-10 was added, and after at least 300 sec, 1 µM ionomycin containing 0.9 M of Calcium chloride (positive control) was added. Fluorescence was quantified using the Bio-format plugin in ImageJ software.

Analysis was performed as depicted in Figure 2.3. Besides the 20 cells selected for analysis, a background reading (a region where there were no cells) was included. The background reading was subtracted from the raw data generated for each cell at the different time points. The background-corrected values were subtracted from the average of the baseline values and converted to a percentage by dividing each value by the highest signal obtained in response to Ionomycin and calcium chloride, and multiplying by 100. The maximum amplitude of calcium

released was calculated by taking the average of the maximum amount of calcium released after the addition of KP-10, for the 20 cells that were selected per cell line. The time of maximum amplitude was calculated by taking the average of the time in which the maximum amplitude was attained for the 20 cells in each of the two independent experiments per cell line.

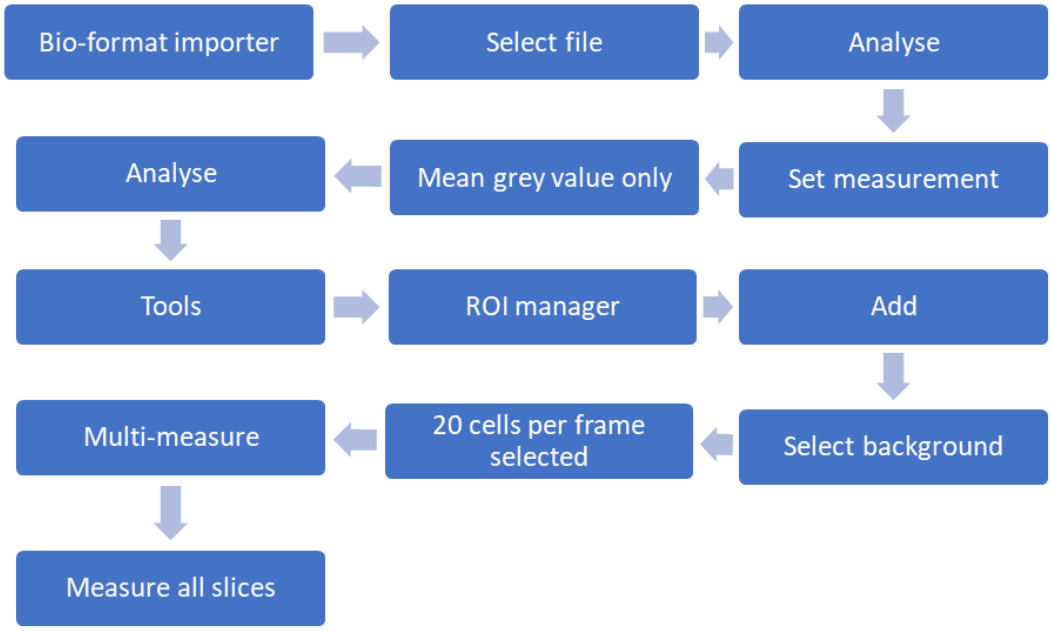

Figure 2.3: Flow-diagram depicting the steps used to generate data from the calcium assay videos using the Bio-format importer on ImageJ.

Chapter 3: Results

3.1 shRNA dependent knockdown of KISS1R expression has no effect on kisspeptin-dependent calcium mobilisation

To investigate how KISS1R mediates its effects on migration in breast cancer cell lines, we decided to modulate its expression. Previous data from our research group showed KISS1R to be active in MDA-MB-231 cells and responsible for increased migration. Thus, we sought to repress expression of KISS1R in this cell line using shRNA to prove that increased migration after KP-10 stimulation was dependent on KISS1R. A lentiviral KISS1R shRNA and shRNA control expression plasmid was previously generated (section 2.1.1.2). To assess the efficiency of the KISS1R shRNA construct, HEK-293T cells were transfected with this construct using XtremeGene^{TM} HP transfection reagent. This was done because these cells are easily transfected and have shown to express KISS1R. 48 h post transfection, RNA was isolated from shRNA control and KISS1R shRNA plasmid transfected cells, first strand cDNA synthesis was performed and the product was subsequently used as template for RT-PCR analysis (Figure 3.1). Primers targeting the KISS1R ORF (lane 2 to 4) were used to amplify KISS1R cDNA while primers targeting a section of the ACTB ORF (lane 5 to 7) (section 2.1.3) were used as a housekeeping control. Resulting product was resolved on an agarose gel and visualised using a DNA stain. Band intensity was quantified and used to determine relative expression of KISS1R in each sample.

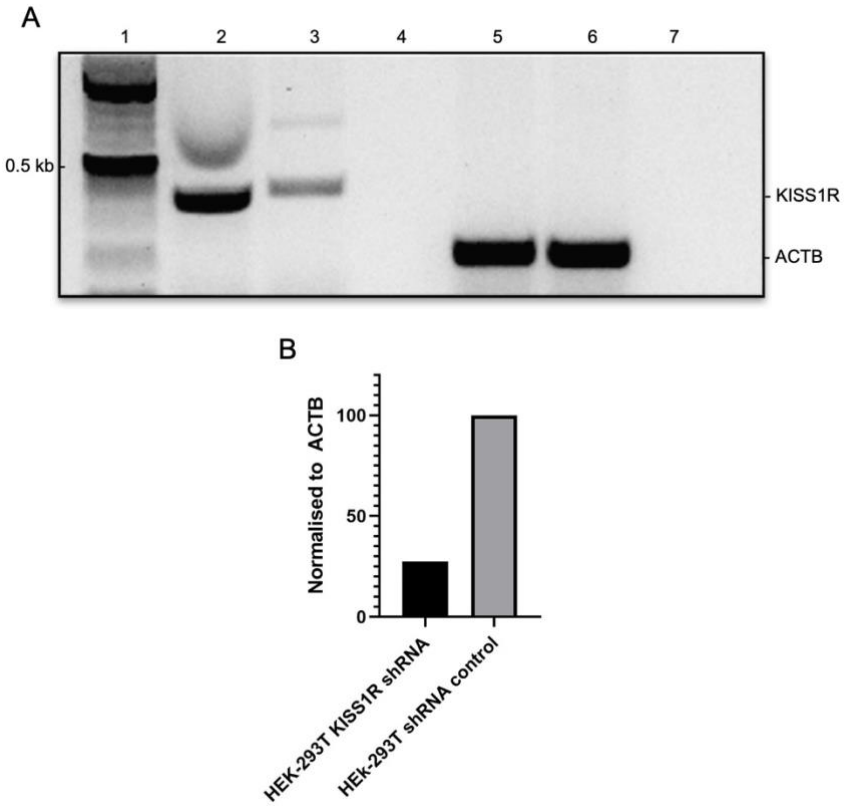

Figure 3.1: RT-PCR demonstrates that shRNA reduces KISS1R mRNA expression in HEK-293T cells.

(A) RT-PCR as performed on cDNA synthesised from extracted mRNA of cells transfected with control shRNA plasmid (lane 2 and 5) and KISS1R shRNA plasmid (lane 3 and 6). Expression of KISS1R mRNA was assessed (lane 2 and 3) and normalised to ACTB expression (lane 5 and 6) from the respective conditions. A 1 Kb plus ladder (lane 1) and negative controls for both KISS1R (lane 4) and ACTB (lane 7) were included. The KISS1R label on the right indicates the amplified KISS1R fragment of the expected size while the ACTB label indicates the amplicon for actin with the expected size. Expected amplicon sizes: KISS1R - 399 base pairs (bp), ACTB – 225 bp. (B) Quantification of relative *KISS1R* mRNA expression in HEK-293T transfected with the KISS1R shRNA plasmid and control shRNA plasmid. n = 1

The results of this experiment show that in control transfected HEK-293T cells, *KISS1R* mRNA is present as shown by the presence of the 399 bp amplicon. However, its expression is reduced by 70% in the cells transfected with the KISS1R shRNA. No significant difference in expression is observed for *ACTB* mRNA (225 bp amplicon) in either cell line suggesting that there is KISS1R specific downregulation of transcription. Thus, the construct is effective and can be used to generate lentiviral particles that can effectively knockdown KISS1R expression in the breast cancer cell line, MDA-MB-231.

Transfection of HEK-293T cells with the KISS1R shRNA construct reduced *KISS1R* mRNA levels, however, as transfections are transient this effect would only last briefly, which would not provide us with the necessary model for this study. To address this, the constructs assessed in the previous experiment were used to generate shRNA-containing lentiviral particles with the aim of generating HEK-293T and MDA-MB-231 cell lines that stably express these shRNA constructs, resulting in continuous knockdown of KISS1R. The lentiviral particles were generated by transfecting HEK-293T cells with the pLKO.1 KISS1R shRNA or control shRNA plasmid, a CMV packaging plasmid and a VSV-G envelope plasmid in ratios described in section 2.3.2.6. The media was changed 12 h post transfection to remove the transfection reagent in preparation for harvesting of the lentiviral particles 48 and 72 h post transfection. Subsequently, HEK-293T and MDA-MB-231 cells were transduced with the lentiviral particles for 24 h, after which cells were placed under puromycin selection until there were no uninfected cells remaining. An uninfected control was included to determine the end point of selection. After selection, RNA was isolated from both cell lines transduced with the control shRNA and KISS1R shRNA lentivirus, and first strand cDNA synthesis performed to provide the template for RT-PCR analysis (Figure 3.2). Primers targeting the KISS1R ORF (lane 2 to 6) and the ACTB ORF (lane 7 to 11) were used to amplify the target regions and DNA fragments were visualised on an agarose gel.

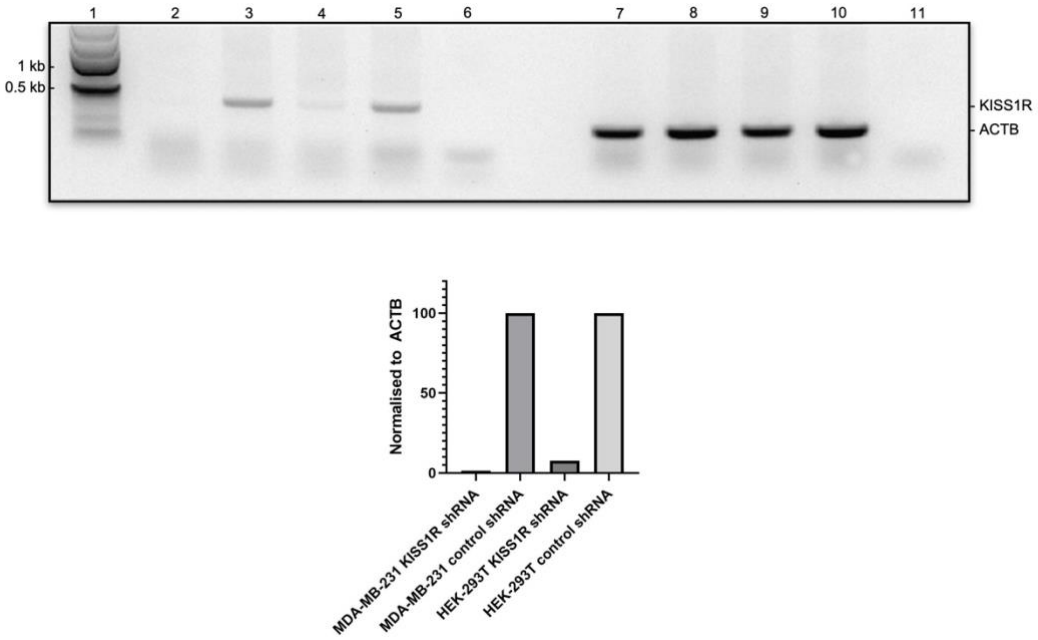

Figure 3.2: RT-PCR demonstrates that shRNA reduces KISS1R mRNA expression in HEK-293T and MDA-MB-231 cells.

(A) RT-PCR as performed on cDNA synthesised from extracted mRNA from MDA-MB-231 cells transduced with lentiviral particles containing either the control shRNA construct (lane 3 and 8) and KISS1R shRNA construct (lane 2 and 7), as well as HEK-293T cells transduced with lentiviral particles containing the control shRNA construct (lane 5 and 10) and the KISS1R shRNA construct (lane 4 and 9). Expression of *KISS1R* mRNA was assessed (lanes 2 to 5) and normalised to ACTB expression (lanes 7 to 10) from the respective conditions. A 1 Kb plus ladder (lane 1) and negative controls for both KISS1R (lane 6) and ACTB (lane 11) were included. The KISS1R label on the right indicates the expected size of the amplified KISS1R fragment, while the ACTB label indicates the expected size of the amplified ACTB fragment. Expected amplicon sizes: *KISS1R* - 399 base pairs (bp), ACTB – 225 bp. (B) Quantification of relative *KISS1R* mRNA expression in MDA-MB-231 and HEK-293T transduced with lentiviral particles containing the KISS1R shRNA construct and control shRNA construct. n = 1

The results of this experiment confirmed the presence of *KISS1R* mRNA in both the MDA-MB-231 and HEK-293T shRNA control cell lines as indicated by the presence of the KISS1R fragment at 339 bp. In the KISS1R shRNA transduced MDA-MB-231 and HEK-293T cell lines a reduction of 99% and 90% was seen respectively. When assessing *ACTB* mRNA (225 bp amplicon) levels between samples, similar levels of expression was observed suggesting that the difference in expression is KISS1R specific, which demonstrates that we were able to generate KISS1R knockdown MDA-MB-231 and HEK-293T cell lines.

It would have been ideal to confirm KISS1R knockdown through western blot analysis, however, we have not been able to confirm that the KISS1R antibodies

available in our laboratory specifically bind to KISS1R. To overcome this limitation we decided to use downstream signalling in response to KP-10 stimulation to assess if we were able to alter KISS1R protein levels. KISS1R belongs to the $G\alpha_{q/11}$ protein family and as explained in section 1.3.3, when stimulated, this receptor activates phospholipase C-β which is responsible for converting PIP_2 into DAG, which activates the ERK 1/2 pathway, and IP_3, which binds to IP_3 receptors in the ER resulting in the release of intracellular calcium. A previous research study in our laboratory had optimised a calcium signalling assay using confocal microscopy, and subsequently confirmed the release of intracellular calcium into the cytosol in response to KP-10 stimulation in the MDA-MB-231 cell line.[92] Therefore, it was decided to use this assay to determine if there was a difference in calcium release between the MDA-MB-231 shRNA control and MDA-MB-231 KISS1R shRNA cell line as a way to assess if any functional KISS1R levels remained in the knockdown cells. KP-10 was administered at a concentration of 100 nm, as it has been shown to be the lowest concentration that is able to stimulate KISS1R, and has been used in previous studies.[59,92] Both cell lines were seeded into a Ibidi plate and left overnight to attach. 24 h after plating, the calcium indicator dye, Fluo-3 Am, was added to each well and the cells were prepared for confocal microscopy as explained by section 2.4.2. After the incubation period, the microslide was put into the chamber of the microscope and the video capture was initiated prior to the addition of KP-10 in order for a baseline fluorescence measurement to be calculated during analysis. After approximately 75 sec, 100 nM of KP-10 was added to each well, and after 350 sec a solution of Ionomycin and calcium chloride (positive control) was added (Figure 3.3).

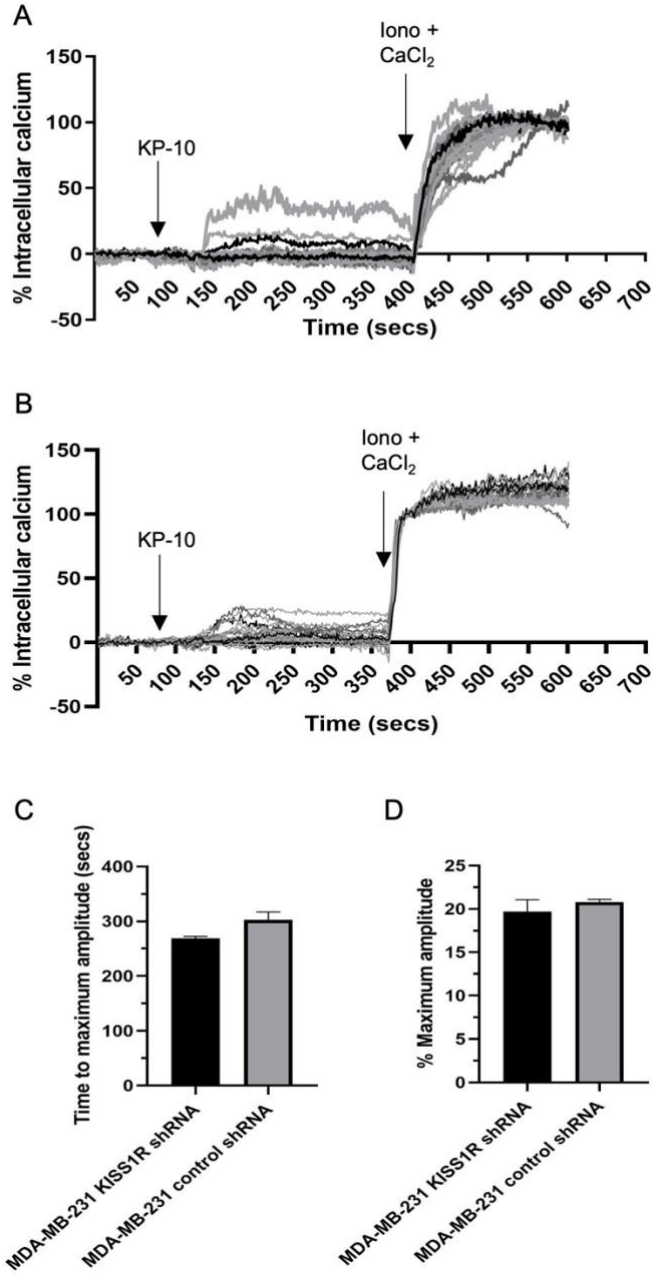

Figure 3.3: shRNA knockdown of KISS1R does not alter intracellular calcium release.

MDA-MB-231 shRNA control and MDA-MB-231 KISS1R shRNA cells were incubated with 2 µM Fluo-3 before being imaged using a Zeiss LSM800 with a 20x objective. Images were taken over 150 ms. KP-10 was added after 75 s and Ionomycin and calcium after at least 250 s. Line traces of individual cells within an experiment showing percentage intracellular calcium mobilisation over time of twenty cells of (A) MDA-MB-231 shRNA control and (B) MDA-MB-231 KISS1R shRNA are shown. (C) The mean ± SEM maximum amplitude for both cell lines from two experiments is shown. (D) Mean ± SEM time to reach maximum calcium release of both cell lines is presented. n = 2

Despite the 99% reduction of *KISS1R* mRNA in the MDA-MB-231 KISS1R shRNA cell line, the magnitude of calcium release in response to KP-10 was similar in the MDA-MB-231 control shRNA and KISS1R shRNA lines (~20%). In addition, the MDA-MB-231 KISS1R shRNA cell line reached maximum calcium release in approximately 275 sec while the MDA-MB-231 control shRNA cell line reached maximum release in 300 sec, with no significant difference between the two cell lines. This result suggests that while we were able to alter the level of *KISS1R* mRNA, this had no effect on the level of KISS1R protein in these cells, therefore showing that we were not be able generate a functional KISS1R knockdown cell line using an shRNA-lentiviral system.

With this line of investigation not providing the appropriate model for this study, we decided to investigate the use of CRISPR-Cas9 gene editing to develop KISS1R KO cell lines.

3.2 Establishing a CRISPR-Cas9 protocol to generate KISS1R KO cell lines

CRISPR-Cas9 gene editing has previously been used to generate KO breast cancer cell lines for proteins such as fatty acid synthase (FASN), C-X-C chemokine receptor 4 and 7 (CXCR4 and CXCR7).[93–95] These articles follow a similar workflow, providing us with a template to conduct a similar path to generate a KISS1R KO cell line. In our method we made use of the CRISPR-Cas9 containing plasmid, pSpCas9(BB)-2A-GFP PX458, which contains a GFP gene, which would allow us to identify and isolate cells where transfection was successful and the plasmid was being expressed. The presence of a selectable marker was vital as transfection efficiencies achieved in breast cancer cell lines are low. Therefore, to increase the chance of identifying a KO single cell clone, we would only assess GFP-positive cells. CRISPOR, a web tool that designs primers and sgRNA for CRISPR-Cas9 experiments was used to design five sgRNA's (Section 2.1.2) that target KISS1R, after which they were synthesized by Integrated DNA Technologies.

3.2.1 Cloning and clone assessment

The cloning strategy followed was described by Addgene as described in section 2.2.2.1. To determine if the selected colonies had the associated sgRNA

successfully inserted into the vector, a PCR was performed using the plasmid screening primer pair (section 2.1.3). An amplicon would only be produced if the vector did not contain the target sgRNA sequence (Figure 3.4). A negative control (water) and a positive control (non-recombinant vector) was included in the analysis.

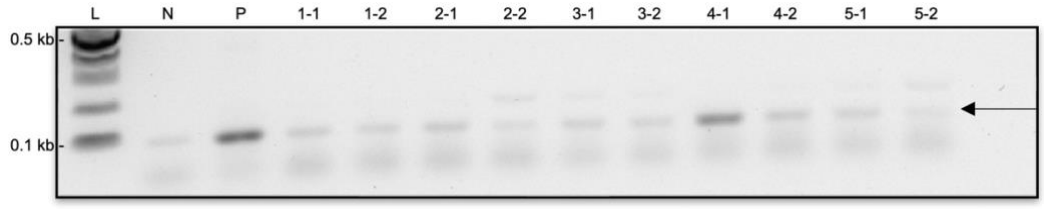

Figure 3.4: All five sgRNA's were successfully cloned into the CRISPR-Cas9 vector.

Two clones for each sgRNA were selected for screening by PCR. Unsuccessful insertion of the sgRNA sequence resulted in a 100 bp amplicon. Numbers indicate sgRNA construct and colony number. L: 1 kb plus ladder, N: Negative control, P: Positive control (non-recombinant vector).

From the resulting agarose gel it is clear that a similar fragment was produced in sgRNA 4 colony 1 (lane 10) when compared to the non-recombinant control in lane 3, showing that we were not successful in inserting the sgRNA in this colony. However, we were successful in the remaining colonies. To ensure that the sgRNAs were inserted correctly and have the correct sequence, all recombinant clones were analysed by Sanger sequencing using the plasmid screening forward primer. DNA sequences were analysed using CLC Main Workbench. The sequencing results were aligned with the corresponding designed sgRNA sequences (Figures 3.5).

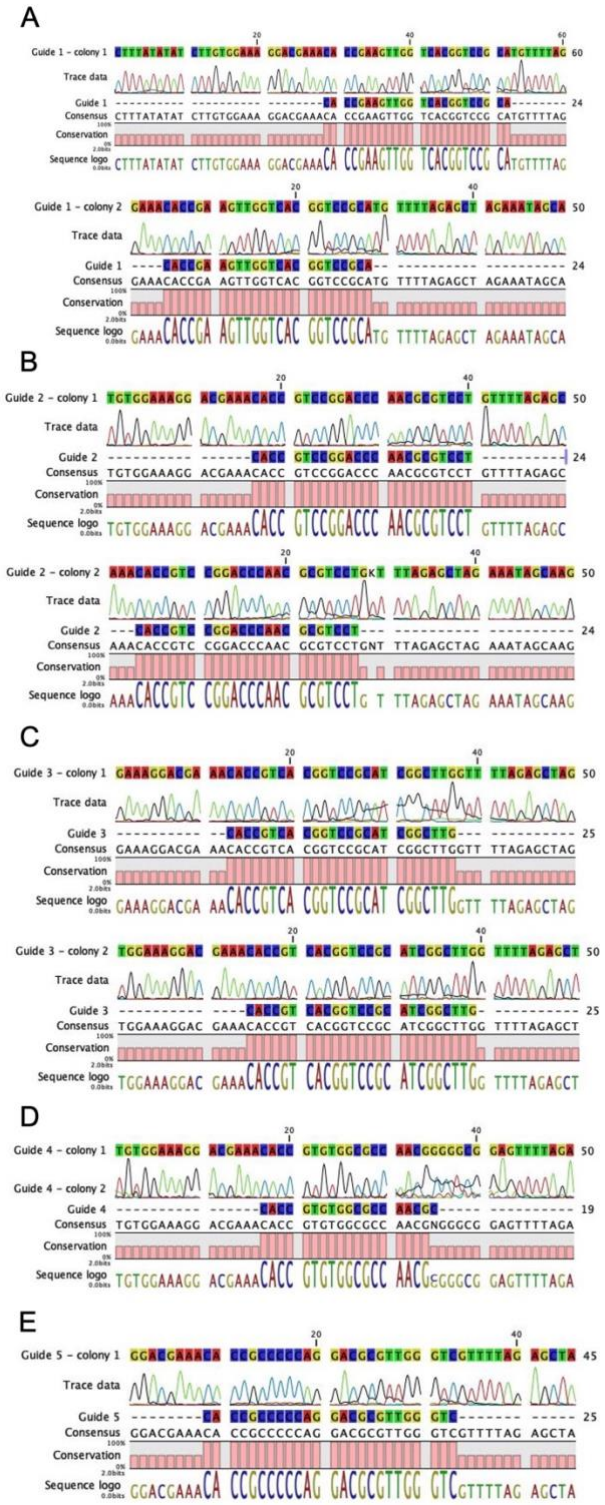

Figure 3.5: Sequencing alignments confirming the insertion of the labelled sgRNA into the CRISPR-Cas9 vector in either one or two clones.

Alignments between the Sanger sequencing traces and the corresponding sgRNA sequences were generated for each recombinant clone using CLC Main workbench. (A) sgRNA 1 (B) sgRNA 2 (C) sgRNA 3 (D) sgRNA 4 (E) sgRNA 5.

The analysis of the sequencing results show that the correct sgRNA sequences were inserted into both clones for sgRNA 1, sgRNA 2, sgRNA 3 and into a single clone of sgRNA 4 and sgRNA 5. sgRNA 5, clone 2 was excluded from the analysis as the quality score was below 25. One clone was selected per sgRNA and used for further experiments. Our analysis shows that we have successfully constructed five CRISPR-Cas9 constructs targeting KISS1R.

3.2.2 Determining the efficiency of different sgRNA's

While five sgRNA constructs were generated, only the two constructs with the highest efficiencies will be used to create the KISS1R KO breast cancer cell line. sgRNA efficiency is normally checked in a cell line that can be transfected with a high efficiency, such as the human embryonic kidney cell line, HEK-293T. To asses sgRNA efficiency HEK-293T cells were transfected with each CRISPR-Cas9 construct containing an sgRNA as described in section 2.3.2.5 and were incubated for 24 h before transfection efficiency was checked by fluorescence microscopy to detect the GFP expressed by the constructs (Figure 3.6).

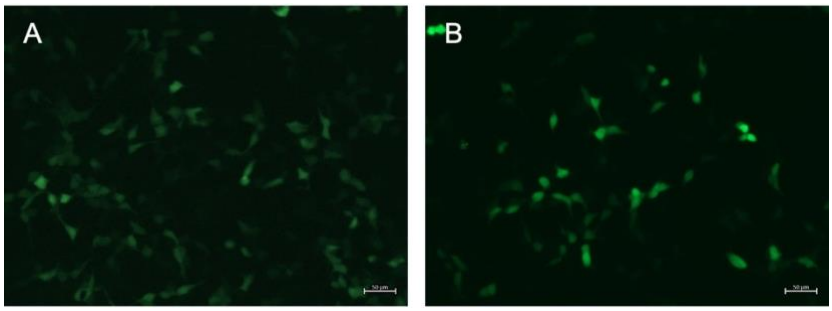

Figure 3.6: HEK-293T cells were effectively transfected with GFP-expressing Cas9 plasmid.

HEK-293T cells were transfected with the CRISPR-Cas9 constructs containing each sgRNA and after 24 h, images were taken using a fluorescent microscope with an x10 objective. Fluorescent images taken of HEK-293T cells transfected with the CRISPR-Cas9 containing sgRNA 1 (A) and 2 (B).

Visual inspection and cell counting of the wells revealed an approximately 70-80% transfection efficiency when comparing the wells under fluorescent and light microscopy.

Cells were harvested 48 h post-transfection and genomic DNA was isolated using the DNA RapidLyse mini-kit. Afterwards, the target region in KISS1R was amplified

by PCR, the double stranded DNA denatured and allowed to re-anneal, to allow hybrid non-matched double strands to form, which were then digested with T7 endonuclease I if present. The percentage of digested fragments relates to the efficiency of the editing of the genome (Figure 3.7).

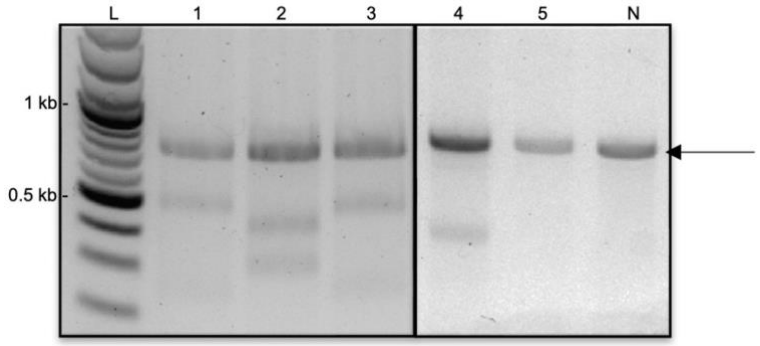

Figure 3.7: Four of the five sgRNA constructs can induce INDEL mutations.

A PCR and T7 endonuclease I digestion was performed and the products resolved on a 1% (w/v) agarose gel. Expected parent amplicon size: 798 bp. Numbers indicate the sgRNA construct. L: 1 kb plus ladder, N: no mutation control. n=1

Table 3.1: INDEL mutation percentages per sgRNA construct.

Guide	Indel Mutation percentage
1	14%
2	20%
3	12%
4	4%

INDEL mutation percentages for each sgRNA construct (Table 3.1) were calculated by quantifying the optical density of the wildtype 798 bp band and the smaller T7 produced bands. The percentage of smaller bands to wildtype band was calculated for each construct as described in section 2.3.2.5. The INDEL mutation percentage was 14% for sgRNA 1, 20% for sgRNA 2, 12% for sgRNA 3, and 4% for the sgRNA 4 construct. sgRNA 5 did not induce an INDEL mutation in these cells and was excluded from further analysis. From these results, we concluded that sgRNA 1 and 2 achieved the highest recombination efficiency in HEK-293T cells and should be used for further cell line generation.

3.2.3 Establishing a single cell cloning strategy using HEK293T cells and guide 2 to create a KO cell line

An important part of establishing a KO cell line is the ability to generate clonal lines by performing single cell cloning. After transfection and selection of GFP-positive cells, these cells need to be diluted so that a single cell can be seeded in each well of a 96 well culture plate. To establish this method in the laboratory, we set up a single cell procedure using HEK-293T cells transfected with the sgRNA 2 construct. While normally one would select GFP-positive cells after transfection using flow cytometry, the equipment we rely on was damaged and inoperable such that this selection step was not possible. Nonetheless, 48 h post transfection, cells were harvested and diluted to a concentration of 20 cells/mL, after which 200 μL, theoretically containing 4 cells, were plated into each well of a 96 well plate. Plates were inspected 48 h after single cell plating and fluorescence microscopy was performed to identify wells containing GFP-positive cells. In most wells attached but round single cells were observed with some wells containing multiple cells up to 4 or 5 (Figure 3.8). None of the cells at this stage appeared to have divided.

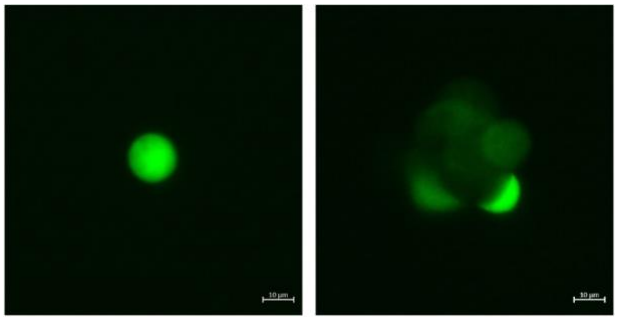

Figure 3.8: GFP-positive cells were successfully isolated using dilutions.

Between 24 and 72 h post-dilution, HEK-293T cells were visualised under a fluorescent microscope using a x40 objective.

Once we confirmed that we were able to isolate single cells using dilutions, HEK-293T cells were transfected, 5x 96 well plates were seeded of which 52 wells contained GFP-positive single cells. The 52 wells containing single positive cells were cultured for a further 2 to 4 weeks, with media being changed every 72 h until the single cells had expanded into large colonies. Due to GFP only being expressed transiently, as well as the difficulty in identifying single cell clones while

they were expanding, light microscopy images were only taken once they had developed into larger colonies. (Figure 3.9).

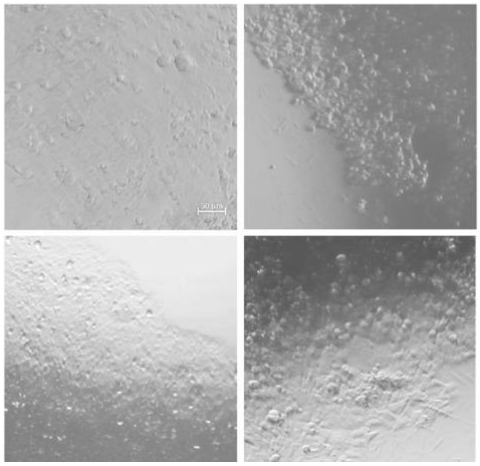

Figure 3.9: Isolated single cells were successfully expanded into colonies.

GFP-positive single cells were expanded until they were large colonies. Images were taken using a x4 objective. The scale bars are the same for all images.

Of the 52 single cell clones, 17 were successfully expanded from which genomic DNA was isolated. PCR with the KISS1R specific primers was performed and the resulting product was denatured, reannealed and then digested using T7 endonuclease I. The products were resolved on 1% agarose gel and visualised (Figure 3.10).

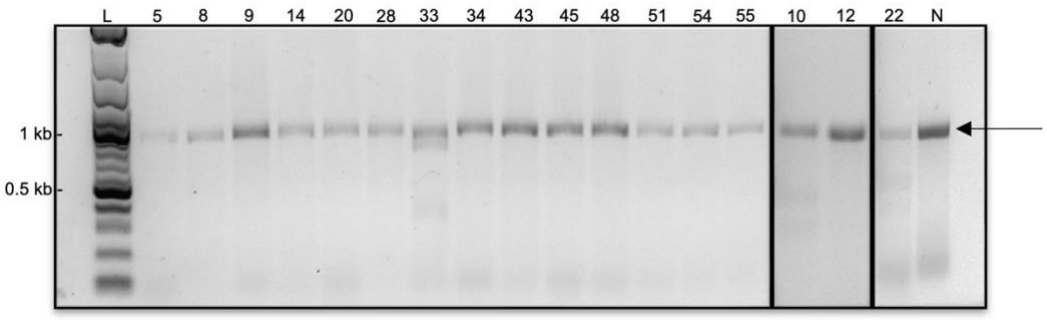

Figure 3.10: HEK-293T clones 10 and 33 were positive for INDEL mutations.

A PCR and T7 endonuclease I digestion was performed on genomic DNA isolated from HEK-293T single cell clones and the products resolved on a 1% (w/v) agarose gel. Expected parent amplicon size: 798 bp Numbers indicate the clone #. L: 1 kb plus ladder, N: No mutation control.

Whilst most of the clones presented with a single DNA fragment at around 800 bp, lanes representing clones 10 and 33 also contained smaller fragments of 450 and 300 bp, and 700 and 300bp, respectively. This data suggests that clones 10 and

33 contain INDEL mutations in the region of interest. Thus, out of 576 single cell clones originally plated, 2 were positive for mutations. This indicates the importance of an initial selection step to isolate only transfected cells for further expansion.

3.2.4 Identifying INDELS in CRISPR gene edited cells

To determine if either clonal cell line harboured INDELs that would result in a KO of KISS1R, Sanger sequencing was performed of the two clones and the control cell line (Figure 3.11 A, B). Resulting sequence traces of the clones and a control were subsequently analysed using Synthego's Inference of CRISPR Edits (ICE) tool to determine the effect of the INDELs, the presence of wildtype sequence and the contribution of different INDEL alleles (Figure 3.11 C, D).

ICE analysis was performed using the target sequence as shown in Table 2.3 for sgRNA 2 and INDEL, R^2 and KO scores were calculated. Analysis is dependent on diploid alleles. The INDEL score, R^2 value and KO score for clone 10 were 94%, 0.94, and 58% respectively (Figure 3.11 C) while for clone 33 the scores were 73%, 0.73, and 72% respectively (Figure 3.11 D). The allele contributions show that for clone 10, 5 separate INDELs were detected of which 3 had deletions of 12 nucleotides, 1 had a deletion of 8 nucleotides and the last an insertion of 1 nucleotide. Thus only 2/5 INDELs would result in a frameshift mutation which is why the KO score is only 58%, while the INDEL score is 94%. In contrast, clone 33 harboured only 3 significant alleles with deletions, one of 24 nucleotides and two of 27 nucleotides. There were a number of additional calculated alleles with contributions of less than 5% which cannot be included as the noise to signal ratio is too low to be able to determine their validity, hence the INDEL score of 73%. However, all 3 major alleles would cause a KO even though one has 24 nucleotides deleted which would not result in a frameshift mutation. This allele has lost more than 21 bp, which statistically is indicated to result in a KO in most cases. The R^2 value of this clone is also only 0.72, which indicates that 27% of the contributing alleles do not fit the model and can therefore be discarded. For both clones it is clear that there are more than 2 alleles in the pool. Since both have at least 3 major contributing alleles, this may indicate polyploidy. Thus, the data suggests that HEK-293T cells are polyploid for the KISS1R locus but neither clones contains the wildtype sequence suggesting that all alleles have been altered through INDELs

with clone 33 having a better KO score suggesting that this clone would act as a functional KO for KISS1R.

A

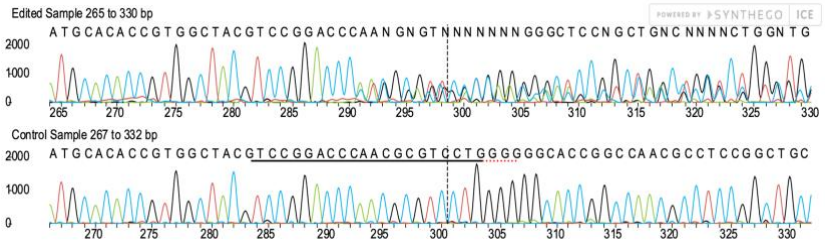

B

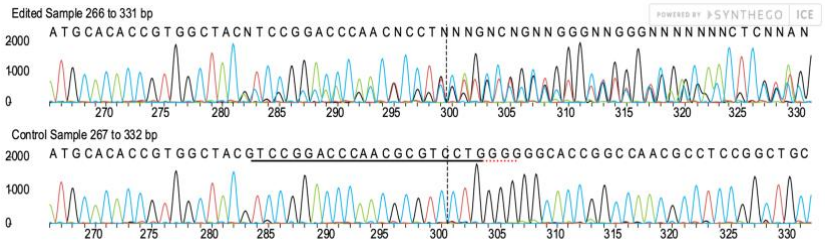

C

D

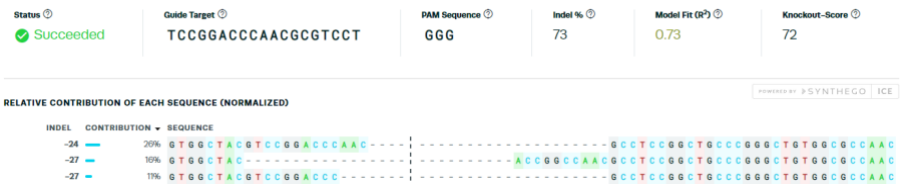

Figure 3.11: Sequencing and ICE analysis of clone 10 and 33 for KISS1R INDELS of sgRNA 2.

Comparison of control versus clone 10 (A) and clone 33 (B) histograms of DNA sequence with the CRISPR target guide sequence underlined in the DNA sequence. C and D represent the allele contribution, INDEL and KO scores of clone 10 (C) and clone 33 (D). Vertical dotted line represents the cut site and number on the left the deletion/insertion size.

Together, this data indicates that we have successfully generated CRISPR-Cas9 constructs and used them to create a KO clonal line in HEK-293T cells. This strategy was thus adapted for use in the target breast cancer cell line.

3.2.5 Establishing a method to efficiently introduce CRISPR plasmid into MDA-MB-231

Transfection rates using liposomal reagents in breast cancer cell lines are not very effective with efficiency rates in the single digits being very common. Electroporation can produce better results, thus we established and optimised an electroporation protocol for delivery of the CRISPR-Cas9 constructs into MDA-MB-231 cells.

Bio-Rad's GenePulser II electroporation device was available for use in our laboratory, but an electroporation method had not been optimised for this cell line. To establish an electroporation protocol an online search for protocols used in breast cancer cell lines was conducted to obtain values for the different parameters that could be tested. To analyse electroporation success we made use of flow cytometry to assess both cell number and cell positivity for GFP expression. A gating profile for cell size and GFP fluorescence was set up using untransfected cells that was used as the negative control for all further analyses (Figure 3.12 A and B). First we established what percentage positivity was possible with a liposomal transfection reagent. Cells were transfected with the liposomal reagent XtremeGene™ and the empty CRISPR-Cas9 plasmid after which cells were grown for 24 hours before being analysed by flow cytometry (Figure 3.12 C and D). The scatter plot indicates that cells were not affected negatively by the transfection as most were similar to untransfected cells. The GFP histogram showed very few cells with only 1.35% of cells being positive. To improve this outcome we established an electroporation protocol through the following optimisation steps (Table 3.3). All experiments were done with 10 µg DNA and 2 million cells in 200 µL electroporation fluid in cuvettes with a 0.2 cm gap. Only single pulses of 16 ms were delivered. In accordance with protocols found online we tested different voltages at high capacitance or alternatively high voltage with different low capacitances as described in Table 3.3.

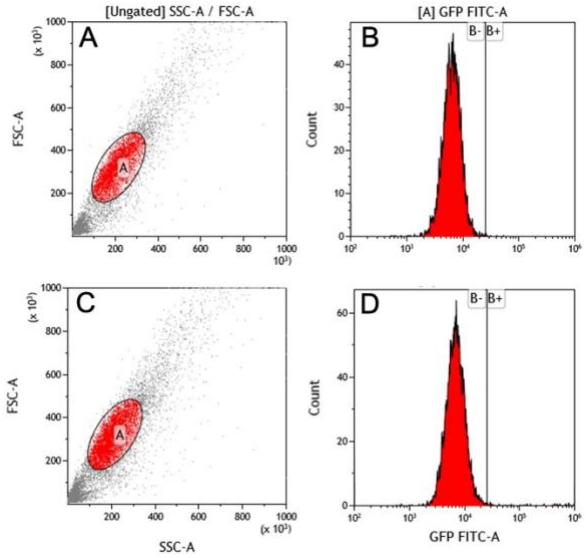

Figure 3.12: Analysis of transfected cells show low transfection efficiency.

MDA-MB-231 cells untransfected (A, B) or transfected with CRISPRCas9-GFP plasmid (C, D) were analysed by flow cytometry. A and C represent scatter plots of forward and side scatter used to identify the viable cells (marked by the circle and red dots). B and D represent the histograms of cells analysed for intensity of fluorescence in the 488 nm channel.

Cells were either electroporated at 140V with different low capacitances ranging between .2 and .3 μF or at different voltages between 110 and 170V at high capacitance of 960 μF. Efficiency was measured by multiplying the percentage cells in population A representing live cells with the percentage of GFP positive cells (Figure 3.13).

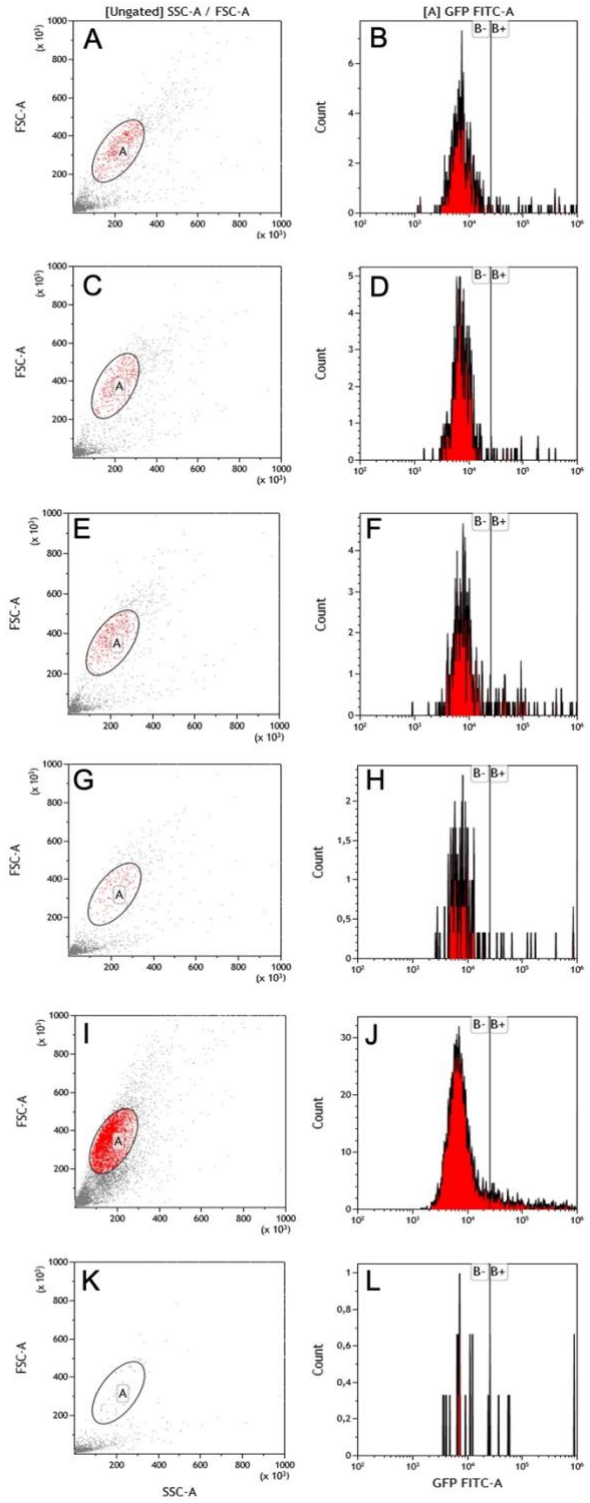

Figure 3.13: Analysis of electroporated cells showed an increase in transfection efficiency.

MDA-MB-231 cells electroporated at 140V 0.25 µF (A,B), 140V 0.3 µF (C,D), 140V 0.25 µF (E,F),110V 960 µF (G,H), 150V 960 µF (I, J), 110V 960 µF (K,L). Left: Scatter plots of forward and side scatter used to identify the viable cells (marked by the circle and red dots). Right: Histograms of cells analysed for intensity of fluorescence in the 488 nm channel.

From the results it is clear that low capacitance only performed slightly better than liposomal transfection but importantly very few cells survived this method with survival between 6.66 and 13.91% vs 32.81% survival for liposomal transfection (Table 3.2). Cells electroporated with high capacitance survived better at 110 and 150V (30.32% and 15.45% respectively), although cells did not survive a high voltage of 170V. Moreover, GFP positivity of 14.14 and 16.81 % were obtained at 110 and 150V. When combining these values 110V at 960 μF present the most efficient method for introducing plasmid into the cells while reducing cell death.

Table 3.2: Statistics generated from cytometric analysis of MDA-MB-231 cells transfected using different protocols.

	Protocol	**Percentage GFP-positive cells in population A**	**Percentage of cells that are in population A**	**Overall efficiency (+%)x(popA%)**
	XtremeGene HP transfection reagent (3:1)	1.35	32.81	44.29
1	140V 0.25 μF	9.09	13.50	122.72
2	140V 0.3 μF	9.79	6.66	65.20
3	140V 0.2 μF	6.17	13.91	85.82
4	110V 960 μF	14.14	30.32	428.72
5	150V 960 μF	16.81	15.45	259.71
6	170V 960 μF	26.92	1.84	49.53

3.2.6 Generating and assessing clonal MDA-MB-231 KO cell lines

Before proceeding with the generation of a MDA-MB-231 KO cell line, we needed to ensure that we could isolate single cells using flow cytometry. To 3 wells in a 96 well plate, 100 (A), 10 (B) and 1 (C) GFP-positive MDA-MB-231 cell/s were sorted using a FACSAria™ Fusion cell sorter. A fluorescent microscope was used to confirm that these different cell numbers were achieved (Figure 3.14).

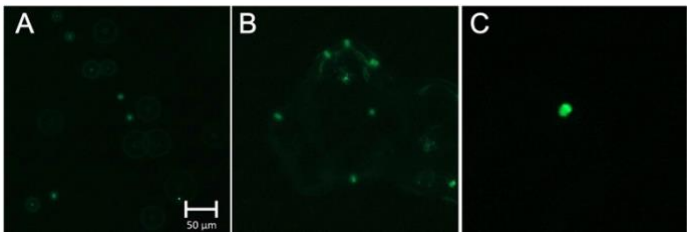

Figure 3.14: Confirmation that we can isolate a single cell using a cell sorter.

GFP-positive MDA-MB-231 cells were sorted at different cell numbers to assess if this cell sorter could successfully sort a single cell into a well and images were taken using a x50 objective. (A) 100 cells (B) 10 cells (C) 1 cell. The scale bars are the same for all images.

With optimised electroporation settings and confirmation of single cell sorting, we could proceed with MDA-MB-231 KO cell line generation. 2 million MDA-MB-231 cells were electroporated with 10 µg of the sgRNA 1 and 2 construct using the optimised settings. After cells were plated back into cell culture flasks they were allowed to attach. GFP expression was confirmed 24 h post-transfection, and after 48 h cells were selected by flow cytometry using either a Cytoflex SRT or FACSAria™ Fusion cell sorter as described in section 2.3.2.8.2 and 2.3.2.8.3. From the 6 million cells electroporated, 28 single cell clones were successfully expanded, followed by genomic DNA extraction. PCR with the KISS1R specific primers was performed as described in section 2.2.2.5. These PCR products were denatured, reannealed and digested using T7 endonuclease I. The final products were resolved on a 1% agarose gel and visualised using a Chemidoc MP system™ (Figure 3.15).

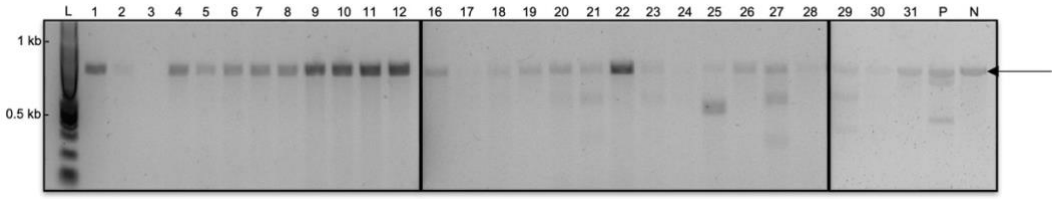

Figure 3.15: T7 endonuclease assay indicates 7 MDA-MB-231 clones contain one or more INDELs.

A PCR followed by T7 endonuclease I digestion was performed and products electrophoresed on a 1% (w/v) agarose gel. Numbers indicate the colony. L: 1 kb plus ladder, P: HEK-293T clone 33 (positive control), N: No mutation control. Expected parent amplicon size: 782 bp. Clones 1-12 are derived from sgRNA 2 transduced cells while clone 16- 31 are derived from sgRNA 1.

No amplicon was visible in clones 3,17 and 24, however an 800 bp product was visible for all the remaining clones confirming successful amplification of the target KISS1R region. A band of approximately 600 bp was present in clones 18,20,21,

23, 27 and 29, a 500 bp fragment was visible in clone 25 and a 400 bp fragment was present in clone 29. In addition, a smaller fragment of 300 bp was present in clones 21 and 27. Lanes with multiple bands indicate clones in which INDEL mutations were inserted into the KISS1R region. The positive control (P) did present multiple bands as expected, therefore confirming the reliability of our result. The remaining clones were negative for an INDEL mutation. Thus, only sgRNA 1 transduced cells harboured any INDELS.

To assess the nature of the INDELs in the seven clones, the target region of each clone was sequenced using Sanger sequencing. Resulting sequence traces of the clone and a control were subsequently analysed using Synthego's ICE tool, and a trace comparison of sequencing data between the wildtype MDA-MB-231 and different clones were generated (Figure 3.16). An INDEL contribution table was generated highlighting the sequences present in each clone and the percentage each contributes to the population (Figure 3.17). ICE analysis of clone 27 failed due to poor sequence results and was excluded from further analysis.

Clone 18 and 20 (A, B) were the only clones with only two predicted deletions of -23 and -1, and -8 and -6 respectively. The -6 deletion in clone 20 would only result in a 2 amino acid deletion and thus is not counted in the KO score which was 49%. The other clones, 21, 23, 25, and 29 (C-F) all had three alleles. However, for clone 23, two of the alleles are a -16 deletion and with only a substitution of a G for C between them it could be that they are actually the same. If true, this would mean clone 23 possesses a +2 and a -16 allele of equal distribution and could potentially be a complete KO due to the frameshift mutations. The same applies to clone 21 (C) with a +1 allele and 2 -11 alleles that are also only different in one nucleotide substitution of G to A. These two alleles contribute 39 and 8% so that together they are close to the expected 50%. Clones 25 (E) and 29 (F) do have three alleles each which are very different from each other with -30, -5, and -1, and -1, -8, -33 deletions in each. Both contain one allele that is a multiple of 3 which would not induce a frameshift mutation (-30 and -33) but these are larger deletions than 21 bp which commonly results in a KO of the target gene. These two clones may constitute more than one parent cell to generate these different alleles since we know that MDA-MB-231 cells only have two alleles of KISS1R. Thus, we have generated at least one and possibly 3 clones that are compound heterozygotes for frameshift mutations in KISS1R that should result in loss of expression. However,

the ICE analysis should be repeated with a more appropriate primer as the primer used was too far from the target site resulting in the orange succeeded signs on the INDEL contribution table analysis (3.17).

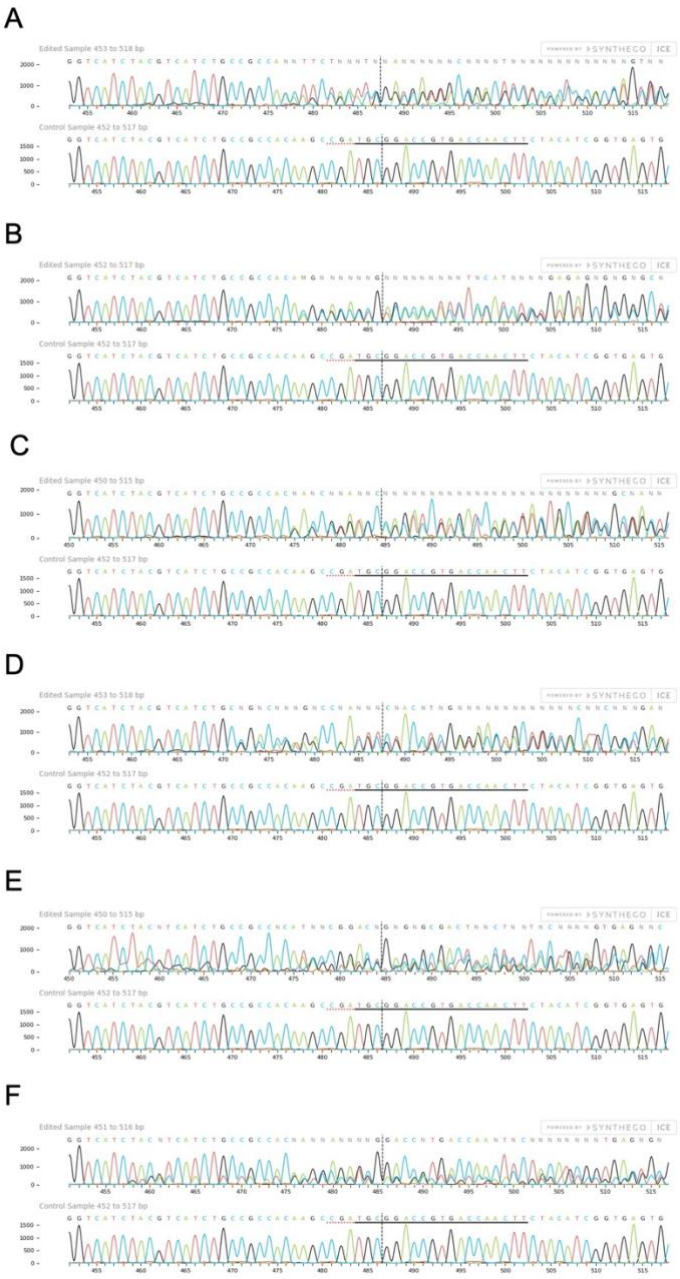

Figure 3.16: Sequencing confirmation of INDEL mutations in MDA-MB-231 single cell clones.

Comparison of control versus 7 single cell clones. Histograms of DNA sequence with the CRISPR target guide sequence underlined in the DNA sequence. (A) Clone 18 (B) Clone 20 (C) clone 21 (D) clone 23 (E) clone 25 (F) clone 29.

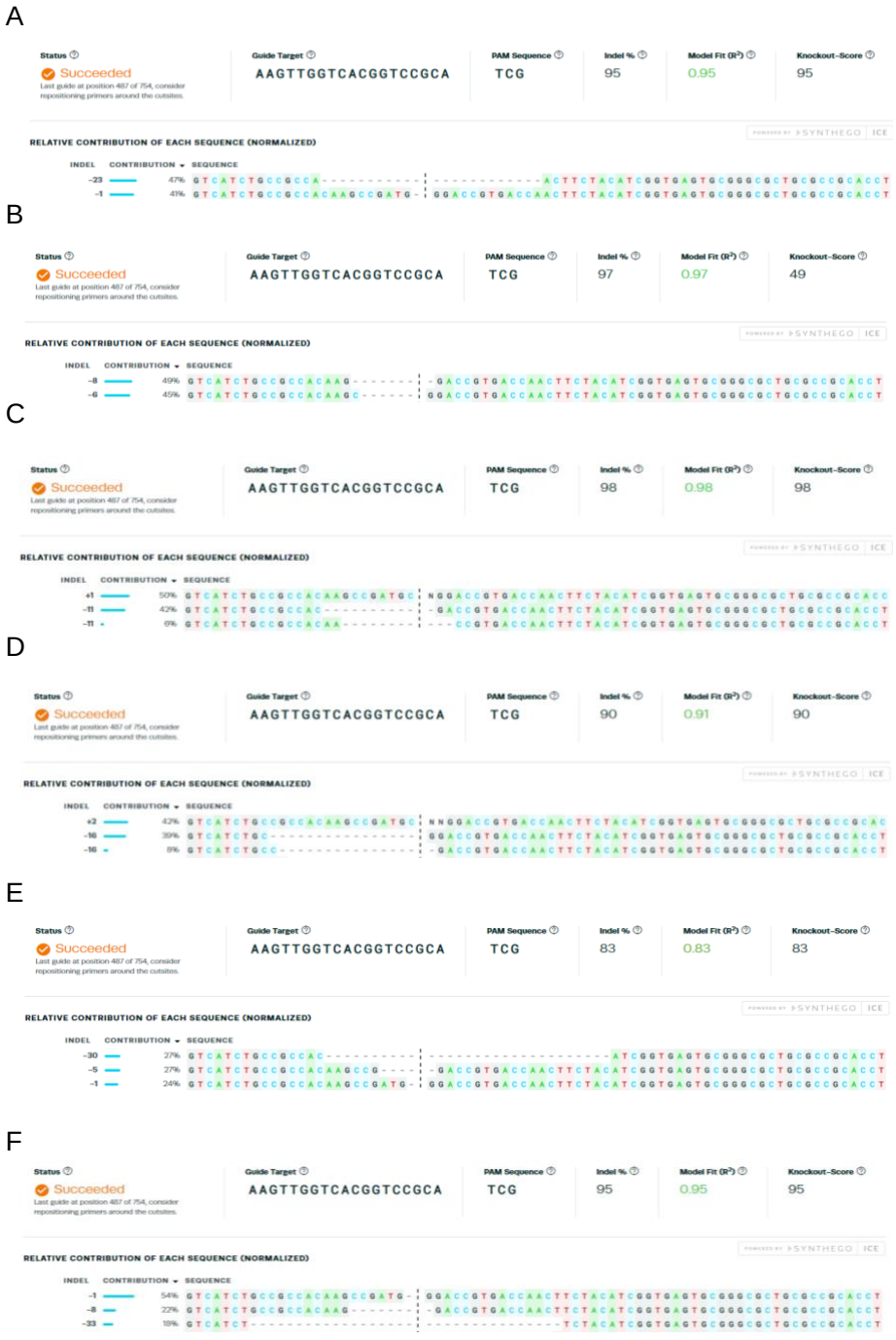

Figure 3.17: Heterozygous and homozygous mutations were inserted in MDA-MB-231 clones.

Sanger sequencing data was analysed using Synthego's ICE analysis tool. INDEL contribution tables were generated for (A) clone 18, (B) clone 20, (C) clone 21, (D) clone 23, (E) clone 25 and (F) clone 27, highlighting the different INDELs present in these populations and their proportions in the edited population.

Chapter 4: Discussion

Kisspeptin, encoded by the KISS-1 gene, was first identified as a metastasis suppressor gene in melanoma cells in 1996.[56] Subtractive hybridization and Northern blot analysis was used to compare mRNA levels in metastatic and non-metastatic melanoma cells. Using this technique, they discovered that *KISS-1* mRNA was only detectable in non-metastatic melanoma cells and concluded that silencing of KISS1R was required for metastasis to occur.[56] A year later, the same scientists showed that the KISS-1 gene also acts as a metastasis suppressor in the cell line MDA-MB-435 suggesting that the loss of KISS-1 is also a prerequisite for breast cancer metastasis.[84] However, it was later shown that MDA-MB-435 cells are actually melanoma cells.[85] Subsequently, a number of studies confirmed that a loss of KISS-1 was correlated to increased metastasis in cancers including prostate cancer[62], bladder cancer[63], gestational trophoblastic disease[64], hepatocellular cancer[65], oesophageal carcinoma[66] and papillary thyroid cancer.[67] Missing from this list is breast cancer since different studies have shown contrasting data with regards to the correlation between KISS-1 expression and metastasis.[86–89] Thus, studying the role of KISS-1 and its receptor in breast cancer is of interest as it is clear there is no clear relationship between expression and metastasis.

Many studies investigating the role of KISS-1 and its receptor KISS1R make use of exogenous overexpression of KISS1R in cell lines. Since most GPCRs are expressed at low levels a fundamental flaw in such studies is the overabundance of the receptor making such cells exquisitely sensitive to ligand and distorting the normal signalling outputs. Previous studies in our lab have investigated the role of endogenous KISS1R in signalling pathways after kisspeptin stimulation to determine if there are differences in output between different TNBC cell lines. This study confirmed the presence of *KISS1R* mRNA in two such cell lines, BT-20 and MDA-MB-231. Further analysis of these cell lines revealed that the two cell lines respond differentially to kisspeptin stimulation with both inducing calcium release but ERK activation only occurring in BT-20 cells while only MDA-MB-231 cells increasing migration[92]. Thus, previous studies suggesting that the observed differences in KISS-1 expression are aligned with the subtype of breast cancer may in fact be incorrect since here it was shown that two TNBC lines behave differently after stimulation. Thus, endogenous KISS1R signalling is complicated further.

It is important to modulate the endogenous expression of KISS1R to be able to determine with confidence that the effects of kisspeptin are indeed specifically mediated by the receptor. For this, one would want to decrease or remove completely the expression of the receptor to determine if the same effects still occur after exposure to kisspeptin. Using shRNA to modulate protein expression has already been used to shed light on proteins in which their functions are unclear. For example, a study looking at the importance of the gene Bmi-1 in embryonic neural stem cell (NSC) self-renewal employed the use of Bmi-1 targeting shRNA. Knockdown of mRNA was confirmed using RT-PCR followed by western blot analysis that demonstrated reduction in protein levels. Knockdown of this protein showed that reduction of Bmi-1 caused defects in embryonic and adult NSCs proliferation and self-renewal, and implicated cell-cycle inhibitor p21 which contrasts previous research which implicated cell-cycle inhibitors p16/p19.[97] Thus, shRNA can be effectively employed to determine the function of proteins in cells *in vitro*.

In this study, we sought to develop a KISS1R shRNA knockdown cell line using MDA-MB-231 cells, to elucidate the role of KISS1R in breast cancer cell progression. We established MDA-MB-231 cells that continuously express KISS1R shRNA with RT-PCR demonstrating a 99% reduction in *KISS1R* mRNA when compared to the shRNA control cell line. To determine if this reduction in mRNA translates to a reduction in protein level we assessed the release of intracellular calcium in response to KP-10 stimulation of both cell lines using a calcium signalling assay. This assay showed that the MDA-MB-231 shRNA KISS1R and shRNA control cell line had a similar maximum response when stimulated by KP-10 at approximately 20% of max, with a response time of 275 sec and 300 sec respectively. This illustrates that while we were able to achieve a 99% knockdown of *KISS1R* using RT-PCR, no change in release of intracellular calcium in response to KP-10 was observed. This data suggests that even with a significant reduction in *KISS1R* mRNA, enough KISS1R protein remains to elicit a response after KP-10 stimulation. It would be prudent to perform the IP_3 accumulation assay to assess IP_3 production in response to KP-10 stimulation, as it occurs prior to calcium release. Alternatively, KP-10 could be eliciting calcium release through an alternative receptor to KISS1R. A drawback in this study was the lack of a sensitive and specific antibody that can detect endogenous protein. Previous attempts in our

group have tried to optimise detection of KISS1R protein but have failed using both commercially available and custom made antibodies.

While shRNA is stably expressed in this lentiviral system, we did detect remaining *KiSS1R* mRNA suggesting that there remains a small pool of KISS1R protein. GPCRs are known to be able to elicit downstream effects even with very small numbers of receptors. Therefore, our data could indicate that even with a good mRNA reduction due to shRNA enough KISS1R remains to activate the pathway leading to calcium release downstream of KISS1R and KP-10. To ensure complete removal of any KISS1R expression, we needed to generate a KO cell line where KISS1R was genetically removed.

CRISPR-Cas9 mediated gene editing has shown great results in determining the function of proteins and the analysis of signalling networks. In 2014, scientists generated a With-No-Lysine kinase 1 (WNK1) KO HEK-293T cell line to assess its role in the activation and phosphorylation of Ste20- and SPS1-related proline alanine-rich kinase (SPAK) and oxidative stress-responsive kinase 1 (OSR1), which are downstream effector kinases responsible for the regulation of sodium-coupled SLC12 cation chloride cotransporters.[98–100] These cotransporters play an important role in the regulation of cell volume, renal tubular salt reabsorption and chloride homeostasis.[101,102] They found that the WNK1 KO cell lines exhibited low baseline SPAK/OSR1 activity and failed to trigger volume increase after hypertonic stress, confirming that WNK1 played an important role in cell volume regulation.[103] Following this, in 2019 CRISPR-Cas9 was used to generate KO $KRas^{G12D}$ mutated pancreatic cancer cell lines to assess how the removal of this mutated protein effects downstream signalling. They showed through western blot analysis that they were able to knock out the mutated version of KRas, with each cell line still expressing wildtype KRas. Downstream signalling analysis of the KO cells showed similar expression levels of ERK, AKT, STAT3, AMPKα and c-MYC to the corresponding wildtype cell lines, showing that they were able to knock out the KRas mutant while maintaining the presence of the wildtype.[104]

In this study, the use of CRISPR-Cas9 first needed to be optimised as it had not previously been performed in our research unit. Due to the low transfection efficiency of MDA-MB-231 cells (our cell line of interest), HEK-293T cells provided

a good model for testing of the different sgRNA constructs due to their high transfection efficiencies.[105] Using liposomal transfection, we achieved 80% or higher transfection efficiencies and identified two sgRNA's with high efficiency in generating NHEJ alleles, namely sgRNA 1 and 2. Clonal selection of GFP-positive HEK-293T cells transfected with sgRNA 2 further led to the identification of two clones that were positive for an INDEL mutation (clone 10 and 33) as demonstrated by the T7 endonuclease assay. Sequencing Inference of CRISPR Edits (ICE) analysis showed that neither clone possessed a wildtype allele. INDEL and KO scores indicate that for clone 10, 3 of the deletions did not cause a frameshift resulting in a much lower KO score, while for clone 33 the INDEL and KO scores were similar suggesting that all INDELs identified would result in a gene KO. The multiple alleles with significant contribution in both clones suggest that either both clones are in fact originating from multiple cells with different genomes or HEK-293T cells possess more than two alleles of the KISS1R gene. Since it is known that HEK-293T cells are polyploid, we assume that indeed this allele is also polyploid. Nonetheless, the absence of a wildtype allele and the presence of multiple frameshift mutations suggests that these two cell clones will have no expression of KISS1R expression.

Having shown that the sgRNA can induce INDELs in HEK-293T cells, we had to first optimise plasmid delivery into MDA-MB-231 cells. Since it was already well established that liposomal delivery would not deliver the required results, we set up and tested different electroporation protocols to achieve a reasonable transfection efficiency while maintaining a high enough cell survival rate. The best results we obtained was 14% positivity with a 30% survival which was subsequently used to generate a pool of sgRNA 1 plasmid transduced cells. GFP-positive single cells were isolated using flow cytometry, and from these cells 28 clones were successfully expanded, of which 7 (edited using sgRNA 1) were positive for an INDEL mutation. After Sanger sequencing and ICE analysis, we could identify one clone that is very likely to be pure and have frameshift mutations in both alleles while another had INDELs in both alleles but one allele would only have two amino acids missing. This clone could still be used if we were to investigate dose dependency of KISS1R. The remaining clones all had more than two alleles with INDELs, although two clones may have only two alleles if the analysis is not completely accurate. Overall, we can conclude that we have

successfully generated multiple MDA-MB-231 cell populations that are knock out for KISS1R.

While Sanger sequencing combined with ICE analysis, indicated that we have different clones likely to be KO for KISS1R, this needs to be confirmed through a cloning and sequencing experiment or by using next generation sequencing (NGS) analysis. Furthermore, NGS analysis of the genome should also be performed on the KO clones to detect any off target INDELs. To prove that we have a functional KO for KISS1R, a calcium assay or IP_3 accumulation assay will be performed in response to KP-10 exposure. Western blot analysis of KISS1R has been tested previously in our group showing that both commercial and custom antibodies were unable to robustly detect endogenous KISS1R. Thus, a functional assay remains the only viable option.

In conclusion, we tested a shRNA strategy using lentiviral delivery to establish stably expressing lines in order to generate a knockdown cell line for KISS1R. While we were successful in producing a line with >90% reduction in *KISS1R* mRNA, this did not lead to a reduction in the functional output of KISS1R stimulation suggesting the reserve pool of KISS1R protein is able to accommodate the signalling demands even under these reduced expression conditions. Thus, we established a gene editing method in our group to not reduce but completely abrogate KISS1R expression. We have successfully generated both HEK-293T and MDA-MB-231 clonal lines with frameshift mutations in all the KISS1R alleles. These will now be used to assess the functional role of KISS1R in MDA-MB-231 cells as a way to investigate the role of kisspeptin and KISS1R in breast cancer metastasis.

References

1. Stadtmauer EA, Fraietta JA, Davis MM, Cohen AD, Weber KL, Lancaster E, et al. CRISPR-engineered T cells in patients with refractory cancer. Science. 2020;367(6481).

2. Carroll D. Genome engineering with zinc-finger nucleases. Genetics. 2011;188(4):773–82.

3. Gaj T, Gersbach C, Barbas C. ZFN, TALEN and CRISPR/Cas-based methods for genome engineering. Trends Biotechnol. 2013;31(7):397–405.

4. Lieber MR, Gu J, Lu H, Shimazaki N, Tsai AG. Nonhomologous DNA End Joining (NHEJ) and Chromosomal Translocations in Humans. Subcell Biochem. 2010;50:279.

5. Weterings E, Van Gent DC. The mechanism of non-homologous end-joining: a synopsis of synapsis. DNA Repair. 2004;3(11):1425–35.

6. Sonoda E, Hochegger H, Saberi A, Taniguchi Y, Takeda S. Differential usage of non-homologous end-joining and homologous recombination in double strand break repair. DNA Repair. 2006;5(9–10):1021–9.

7. Li H, Yang Y, Hong W, Huang M, Wu M, Zhao X. Applications of genome editing technology in the targeted therapy of human diseases: mechanisms, advances and prospects. Signal Transduct Target Ther. 2020;5(1).

8. Ishino Y, Shinagawa H, Makino K, Amemura M, Nakatura A. Nucleotide sequence of the iap gene, responsible for alkaline phosphatase isozyme conversion in Escherichia coli, and identification of the gene product. J Bacteriol. 1987;169(12):5429.

9. Mojica F, DõÂez-VillasenÄor C, Soria E, Juez G. Biological significance of a family of regularly spaced repeats in the genomes of Archaea, Bacteria and mitochondria. Mol. Microbiol. 2000;36(1):244–6.

10. Jansen R, van Embden J, Gaastra W, Schouls LM. Identification of genes that are associated with DNA repeats in prokaryotes. Mol. Microbiol. 2002;43:1565–75.

11. Pourcel C, Salvignol G, Vergnaud G. CRISPR elements in Yersinia pestis acquire new repeats by preferential uptake of bacteriophage DNA, and provide additional tools for evolutionary studies. Microbiology. 2005;151(3):653–63.

12. Mojica FJM, Díez-Villaseñor C, García-Martínez J, Soria E. Intervening sequences of regularly spaced prokaryotic repeats derive from foreign genetic elements. J Mol Evol. 2005;60(2):174–82.

13. Bolotin A, Quinquis B, Sorokin A, Dusko Ehrlich S. Clustered regularly interspaced short palindrome repeats (CRISPRs) have spacers of extrachromosomal origin. Microbiology. 2005;151(8):2551–61.

14. Barrangou R, Fremaux C, Deveau H, Richardss M, Boyaval P, Moineau S, et al. CRISPR Provides Acquired Resistance Against Viruses in Prokaryotes. Science. 2007;315(3):1709–12.

15. Jinek M, Chylinski K, Fonfara I, Hauer M, Doudna JA, Charpentier E. A programmable dual-RNA-guided DNA endonuclease in adaptive bacterial immunity. Science. 2012;337(6096):816–21.

16. Makarova KS, Grishin N V., Shabalina SA, Wolf YI, Koonin E V. A putative RNA-interference-based immune system in prokaryotes: Computational analysis of the predicted enzymatic machinery, functional analogies with eukaryotic RNAi, and hypothetical mechanisms of action. Biol Direct. 2006;1:1–26.

17. Makarova KS, Aravind L, Wolf YI, Koonin E V. Unification of Cas protein families and a simple scenario for the origin and evolution of CRISPR-Cas systems. Biol Direct. 2011;6:1–27.

18. Makarova KS, Haft DH, Barrangou R, Brouns SJJ, Charpentier E, Horvath P, et al. Evolution and classification of the CRISPR-Cas systems. Nat Rev Microbiol. 2011;9(6):467.

19. Collias D, Beisel CL. CRISPR technologies and the search for the PAM-free nuclease. Nat Commun. 2021;12(1):1–12.

20. Janik E, Niemcewicz M, Ceremuga M, Krzowski L, Saluk-Bijak J, Bijak M. Various aspects of a gene editing system—crispr–cas9. Int J Mol Sci. 2020;21(24):1–20.

21. Ma CC, Wang ZL, Xu T, He ZY, Wei YQ. The approved gene therapy drugs worldwide: from 1998 to 2019. Biotechnol Adv. 2020;40:107502.

22. Esrick EB, Lehmann LE, Biffi A, Achebe M, Brendel C, Ciuculescu MF, et al. Post-Transcriptional Genetic Silencing of BCL11A to Treat Sickle Cell Disease . N Engl J Med. 2021;384(3):205–15.

23. Frangoul H, Altshuler D, Cappellini MD, Chen YS, Domm J, Eustace BK, et al. CRISPR-Cas9 Gene Editing for Sickle Cell Disease and β-Thalassemia. N Engl J Med. 2021;384(3):252–60.

24. Gloriam DE, Fredriksson R, Schiöth HB. The G protein-coupled receptor subset of the rat genome. Genomics. 2007;8:1–17.

25. Melmed S, Koenig R, Rosen C, Auchus R, Goldfin A. Williams Textbook of Endocrinology. 14th ed. Elsevier; 2019.

26. Fredriksson R, Lagerström MC, Lundin LG, Schiöth HB. The G-protein-coupled receptors in the human genome form five main families. Phylogenetic analysis, paralogon groups, and fingerprints. Mol Pharmacol. 2003;63(6):1256–72.

27. Laschet C, Dupuis N, Hanson J. The G protein-coupled receptors deorphanization landscape. Biochem Pharmacol. 2018;153:62–74.

28. Sriram K, Insel PA. G protein-coupled receptors as targets for approved drugs: How many targets and how many drugs? Mol Pharmacol. 2018;93(4):251–8.

29. Schertler GFX, Villa C, Henderson R. Projection structure of rhodopsin. Nature.1993;362(6422):770–2.

30. Dohlman HG, Thorner J, Caron MG, Lefkowitz RJ. Model systems for the

study of seven-transmembrane-segment receptors. Annu Rev Biochem. 1991;60:653–88.

31. Pierce KL, Premont RT, Lefkowitz RJ. Seven-transmembrane receptors. Nat Rev Mol Cell Biol. 2002;3(9):639–50.

32. Odoemelam CS, Percival B, Wallis H, Chang MW, Ahmad Z, Scholey D, et al. G-Protein coupled receptors: structure and function in drug discovery. RSC Adv. 2020;10(60):36337–48.

33. Schiöth HB, Fredriksson R. The GRAFS classification system of G-protein coupled receptors in comparative perspective. Gen Comp Endocrinol. 2005;142:94–101.

34. Schiöth HB, Lagerström MC. Structural diversity of g protein-coupled receptors and significance for drug discovery. Nat Rev Drug Discov. 2008;7(4):339–57.

35. Engelhardt S, Rochais F. G proteins: More than transducers of receptor-generated signals? Circ Res. 2007;100(8):1109–11.

36. Calebiro D, Koszegi Z, Lanoiselée Y, Miljus T, O'Brien S. G protein-coupled receptor-G protein interactions: a single-molecule perspective. Physiol Rev. 2021;101(3):857–906.

37. Wettschureck N, Offermanns S. Mammalian G proteins and their cell type specific functions. Physiol Rev. 2005;85(4):1159–204.

38. Rodbell M. The role of hormone receptors and GTP-regulatory proteins in membrane transduction. Nature. 1980;284(5751):17–22.

39. Mizuno N, Itoh H. Functions and regulatory mechanisms of Gq-signaling pathways. Neurosignals. 2009;17(1):42–54.

40. He W, Danilova V, Zou S, Hellekant G, Max M, Margolskee RF, et al. Partial Rescue of Taste Responses of α-Gustducin Null Mice byTransgenic Expression of α-Transducin. Chem Senses. 2002;27(8):719–27.

41. Siehler S. Regulation of RhoGEF proteins by G12/13-coupled receptors. Br J Pharmacol. 2009;158(1):41.

42. Tang WJ, Gilman AG. Type-Specific Regulation of Adenylyl Cyclase by G Protein βγ Subunits. Science. 1991;254(5037):1500–3.

43. Boyer JL, Waldo GL, Harden TK. Beta gamma-subunit activation of G-protein-regulated phospholipase C. J Biol Chem. 1992;267(35):25451–6.

44. Logothetis DE, Kurachi Y, Galper J, Neer EJ, Clapham DE. The beta gamma subunits of GTP-binding proteins activate the muscarinic K+ channel in heart. Nature. 1987;325(6102):321–6.

45. Stephens L, Smrcka A, Cooke FT, Jackson TR, Sternweis PC, Hawkins PT. A novel phosphoinositide 3 kinase activity in myeloid-derived cells is activated by G protein βγ subunits. Cell. 1994 Apr 8;77(1):83–93.

46. Alhosaini K, Azhar A, Alonazi A, Al-Zoghaibi F. GPCRs: The most promiscuous druggable receptor of the mankind. Saudi Pharm J. 2021;29(6):539–51.

47. Cordeaux Y, Hill SJ. Mechanisms of Cross-Talk between G-Protein-Coupled Receptors. Neurosignals. 2002;11(1):45–57.

48. Bhattacharyya R, Banerjee J, Khalili K, Wedegaertner PB. Differences in Gα12- and Gα13-mediated plasma membrane recruitment of p115-RhoGEF. Cell Signal. 2009;21(6):996–1006.

49. Heasman SJ, Ridley AJ. Mammalian Rho GTPases: new insights into their functions from in vivo studies. Nat Rev Mol Cell Biol. 2008;9(9):690–701.

50. Kobilka BK. G Protein Coupled Receptor Structure and Activation. Biochim Biophys Acta. 2007;1768(4):794.

51. Shenoy SK, Lefkowitz RJ. B-Arrestin-Mediated Receptor Trafficking and Signal Transduction. Trends Pharmacol Sci. 2011;32(9):521–33.

52. Penela P, Ribas C, Mayor F. Mechanisms of regulation of the expression and function of G protein-coupled receptor kinases. Cell Signal. 2003;15(11):973–81.

53. McDonald PH, Chow CW, Miller WE, Laporte SA, Field ME, Lin FT, et al. β-Arrestin 2: A Receptor-Regulated MAPK Scaffold for the Activation of JNK3. Science. 2000:1574–7.

54. Hullmann JE, Grisanti LA, Makarewich CA, Gao E, Gold JI, Chuprun JK, et al. GRK5-mediated exacerbation of pathological cardiac hypertrophy involves facilitation of nuclear NFAT activity. Circ Res. 2014;115(12):976–85.

55. Wu JH, Goswami R, Cai X, Exum ST, Huang X, Zhang L, et al. Regulation of the platelet-derived growth factor receptor-beta by G protein-coupled receptor kinase-5 in vascular smooth muscle cells involves the phosphatase Shp2. J Biol Chem. 2006;281(49):37758–72.

56. Lee JH, Miele ME, Hicks DJ, Phillips KK, Trent J, Weissman B, et al. KiSS-1, a Novel Human Malignant Melanoma Metastasis-Suppressor Gene. J Natl Cancer Inst. 1996;88(23):1731-7

57. Muir AI, Chamberlain L, Elshourbagy NA, Michalovich D, Moore DJ, Calamari A, et al. AXOR12, a Novel Human G Protein-coupled Receptor, Activated by the Peptide KiSS-1. J Biol Chem. 2001;276(31):28969–75.

58. Gahete MD, Vázquez-Borrego MC, Martínez-Fuentes AJ, Tena-Sempere M, Castaño JP, Luque RM. Role of the Kiss1/Kiss1r system in the regulation of pituitary cell function. Mol Cell Endocrinol. 2016;438:100–6.

59. Ke R, Ma X, Lee LTO. Understanding the functions of kisspeptin and kisspeptin receptor (Kiss1R) from clinical case studies. Peptides. 2019;120:170019.

60. Clarke SA, Dhillo WS. Kisspeptin across the human lifespan:evidence from animal studies and beyond. J Endocrinol. 2016;229(3):R83–98.

61. De Tassigny XDA, Fagg LA, Dixon JPC, Day K, Leitch HG, Hendrick AG, et al. Hypogonadotropic hypogonadism in mice lacking a functional Kiss1 gene. Proc Natl Acad Sci. 2007;104(25):10714–9.

62. Wang H, Jones J, Turner T, He QP, Hardy S, Grizzle WE, et al. Clinical

and Biological Significance of KISS1 Expression in Prostate Cancer. Am J Pathol. 2012;180(3):1170.

63. Sanchez-Carbayo M, Capodieci P, Cordon-Cardo C. Tumor Suppressor Role of KiSS-1 in Bladder Cancer : Loss of KiSS-1 Expression Is Associated with Bladder Cancer Progression and Clinical Outcome. Am J Pathol. 2003;162(2):609.

64. Dhillo WS, Savage P, Murphy KG, Chaudhri OB, Patterson M, Nijher GM, et al. Plasma kisspeptin is raised in patients with gestational trophoblastic neoplasia and falls during treatment. Am J Physiol - Endocrinol Metab. 2006;291(5):878–84.

65. Ikeguchi M, Hirooka Y, Kaibara N. Quantitative reverse transcriptase polymerase chain reaction analysis for KiSS-1 and orphan G-protein-coupled receptor (hOT7T175) gene expression in hepatocellular carcinoma. J Cancer Res Clin Oncol. 2003;129(9):531–5.

66. Ikeguchi M, Yamaguchi KI, Kaibara N. Clinical Significance of the Loss of KiSS-1 and Orphan G-Protein-Coupled Receptor (hOT7T175) Gene Expression in Esophageal Squamous Cell Carcinoma.Clin. Cancer Res. 2004;10(4):1379-83

67. Ringel MD, Hardy E, Bernet VJ, Burch HB, Schuppert F, Burman KD, et al. Metastin receptor is overexpressed in papillary thyroid cancer and activates MAP kinase in thyroid cancer cells. J Clin Endocrinol Metab. 2002;87(5):2399–2399.

68. World Health Organization. [Internet] Cancer. [cited 2021 Oct 21]. Available from: https://www.who.int/health-topics/cancer#tab=tab_1

69. Bray F, Soerjomataram I. The Changing Global Burden of Cancer: Transitions in Human Development and Implications for Cancer Prevention and Control. In: Gelband H,Jha P, Sankaranarayanan R, editors. Cancer: Disease Control Priorities. Washington: The World Bank. 2015;p.23–44.

70. Sarkar S, Horn G, Moulton K, Oza A, Byler S, Kokolus S, et al. Cancer Development, Progression, and Therapy: An Epigenetic Overview. Int J Mol Sci. 2013 Oct;14(10):21087.

71. Debela DT, Muzazu SG, Heraro KD, Ndalama MT, Mesele BW, Haile DC, et al. New approaches and procedures for cancer treatment: Current perspectives. SAGE Open Med. 2021;9:205031212110343.

72. Brown G. Oncogenes, Proto-Oncogenes, and Lineage Restriction of Cancer Stem Cells. Int J Mol Sci. 2021 Sep 1;22(18).

73. Wang LH, Wu CF, Rajasekaran N, Shin YK. Loss of Tumor Suppressor Gene Function in Human Cancer: An Overview. Cell Physiol Biochem. 2018;51(6):2647–93.

74. Cooper GM. The Development and Causes of Cancer. The Cell: A Molecular approach.Boston: Sinauer Associates; 2000

75. Sinha T. Tumors: Benign and Malignant. Cancer Ther Oncol Int J. 2018 ;10(3).

76. Sung H, Ferlay J, Siegel RL, Laversanne M, Soerjomataram I, Jemal A, et

al. Global Cancer Statistics 2020: GLOBOCAN Estimates of Incidence and Mortality Worldwide for 36 Cancers in 185 Countries. CA Cancer J Clin. 2021;71(3):209–49.

77. Orrantia-Borunda E, Anchondo-Nuñez P, Acuña-Aguilar L, Gómez-Valles F, Ramírez-Valdespino C. Subtypes of Breast Cancer. In: Mayrovitz H, editor. Breast Cancer. Exon Publications; 2022.

78. Quirke VM. Tamoxifen from Failed Contraceptive Pill to Best-Selling Breast Cancer Medicine: A Case-Study in Pharmaceutical Innovation. Front Pharmacol. 2017;8(9):620.

79. Li ZH, Hu PH, Tu JH, Yu NS. Luminal B breast cancer: patterns of recurrence and clinical outcome. Oncotarget. 2016;7(40):65024.

80. Noone A, Howlader N, Krapcho M, Miller D, Brest A, Yu M, et al. Cancer Statistics Review, 1975-2015 - SEER Statistics. Bethesda; National Cancer Institute;2015

81. Patanaphan V, Salazar O, Risco R. Breast cancer: metastatic patterns and their prognosis. South Med J. 1988;81(9):1109–12.

82. Valastyan S, Weinberg RA. Tumor Metastasis: Molecular Insights and Evolving Paradigms. Cell. 2011;147(2):275–92.

83. Fidler IJ. The pathogenesis of cancer metastasis: the “seed and soil” hypothesis revisited. Nat Rev Cancer. 2003;3(6):453–8.

84. Lee J, Welch G. Suppression of metastasis in human breast carcinoma MDA-MB-435 cells after transfection with the metastasis suppressor gene, KiSS-1. Cancer Res. 1997;57(12):2384–7.

85. Rae JM, Creighton CJ, Meck JM, Haddad BR, Johnson MD. MDA-MB-435 cells are derived from M14 melanoma cells--a loss for breast cancer, but a boon for melanoma research. Breast Cancer Res Treat. 2007 ;104(1):13–9.

86. Kostadima L, Pentheroudakis G, Pavlidis N. The missing kiss of life: Transcriptional activity of the metastasis suppressor gene KiSS1 in early breast cancer. Anticancer Res. 2007;27(4):2499–504.

87. Stark AM, Tongers K, Maass N, Mehdorn HM, Held-Feindt J. Reduced metastasis-suppressor gene mRNA-expression in breast cancer brain metastases. J Cancer Res Clin Oncol. 2005;131(3):191–8.

88. Martin TA, Watkins G, Jiang WG. KiSS-1 expression in human breast cancer. Clin Exp Metastasis. 2005;22(6):503–11.

89. Blake A, Dragan M, Tirona RG, Hardy DB, Brackstone M, Tuck AB, et al. G protein-coupled KISS1 receptor is overexpressed in triple negative breast cancer and promotes drug resistance. Nat Publ Gr. 2017;7:1–17.

90. Concordet JP, Haeussler M. CRISPOR: intuitive guide selection for CRISPR/Cas9 genome editing experiments and screens. Web Serv issue Publ online. 2018;46.

91. Kerschgens K. Considerations for T7 Endonuclease I T7EI mismatch assays [Internet]. [cited 2023 Jan 19]. Available from:

https://horizondiscovery.com/en/resources/featured-articles/considerations-for-t7-endonuclease-i-t7ei-mismatch-assays

92. Azubuike UF, Newton CL, van den Bout I. Lack of Oestrogen Receptor Expression in Breast Cancer Cells Does Not Correlate with Kisspeptin Signalling and Migration. Int J Mol Sci. 2022;23: 8744

93. Gonzalez-Salinas F, Rojo R, Martinez-Amador C, Herrera-Gamboa J, Trevino V. Transcriptomic and cellular analyses of CRISPR/Cas9-mediated edition of FASN show inhibition of aggressive characteristics in breast cancer cells. Biochem Biophys Res Commun. 2020;529(2):321–7.

94. Álvarez-Fernández M, Sanz-Flores M, Sanz-Castillo B, Salazar-Roa M, Partida D, Zapatero-Solana E, et al. Therapeutic relevance of the PP2A-B55 inhibitory kinase MASTL/ Greatwall in breast cancer. Cell Death Differ. 2018;25:828–40.

95. Yang M, Zeng C, Li P, Qian L, Ding B, Huang L, et al. Impact of CXCR4 and CXCR7 KO by CRISPR/Cas9 on the function of triple-negative breast cancer cells. Onco Targets Ther. 2019;12:3849.

96. Szereszewski JM, Pampillo M, Ahow MR, Offermanns S, Bhattacharya M, Babwah A V. GPR54 Regulates ERK1/2 Activity and Hypothalamic Gene Expression in a Gαq/11 and β-Arrestin-Dependent Manner. PLoS One. 2010;5(9):12964.

97. Fasano CA, Dimos JT, Ivanova NB, Lowry N, Lemischka IR, Temple S. shRNA Knockdown of Bmi-1 Reveals a Critical Role for p21-Rb Pathway in NSC Self-Renewal during Development. Cell Stem Cell. 2007;1(1):87–99.

98. Welling PA, Chang YPC, Delpire E, Wade JB. Multigene kinase network, kidney transport, and salt in essential hypertension. Kidney Int. 2010;77(12):1063–9.

99. Vitari AC, Deak M, Morrice NA, Alessi DR. The WNK1 and WNK4 protein kinases that are mutated in Gordon's hypertension syndrome phosphorylate and activate SPAK and OSR1 protein kinases. Biochem J. 2005;391:17–24.

100. Moriguchi T, Urushiyama S, Hisamoto N, Iemura SI, Uchida S, Natsume T, et al. WNK1 regulates phosphorylation of cation-chloride-coupled cotransporters via the STE20-related kinases, SPAK and OSR1. J Biol Chem. 2005 ;280(52):42685–93.

101. Ginns SM, Knepper MA, Ecelbarger CA, Terris J, He X, Coleman RA, et al. Immunolocalization of the secretory isoform of Na-K-Cl cotransporter in rat renal intercalated cells. J Am Soc Nephrol. 1996;7(12):2533–42.

102. Gamba G. Molecular physiology and pathophysiology of electroneutral cation-chloride cotransporters. Physiol Rev. 2005;85(2):423–93.

103. Roy A, Goodman JH, Begum G, Donnelly BF, Pittman G, Weinman EJ, et al. Generation of WNK1 KO cell lines by CRISPR/Cas-mediated genome editing. Am J Physiol - Ren Physiol. 2015;308(4):F366. A

104. Lentsch E, Li L, Pfeffer S, Ekici AB, Taher L, Pilarsky C, et al.

CRISPR/Cas9-Mediated Knock-Out of KrasG12D Mutated Pancreatic Cancer Cell Lines. Int J Mol Sci. 2019; 20(22):5706.

105. Ooi A, Wong A, Esau L, Lemtiri-Chlieh F, Gehring C. A guide to transient expression of membrane proteins in HEK-293 cells for functional characterization. Front Physiol. 2016;7:300.

Appendices

Appendix A: Statistical clearance letter

UNIVERSITEIT VAN PRETORIA
UNIVERSITY OF PRETORIA
YUNIBESITHI YA PRETORIA

Faculty of Health Sciences
Department of Immunology

Letter of Statistical Clearance

Wednesday, June 09, 2021

This letter is to confirm that the MSc student with the Name: **Ms A Marais**, Student No: **17180717** studying at the University of Pretoria discussed the project with the title; **Assessing the role of the KISS1 receptor in breast cancer cell behaviour with the use of CRISPR-mediated gene editing** with me.

I hereby confirm that I am aware of the project and the statistical analysis described and the data generated for the project is appropriate for achieving the research aims.

Yours sincerely

Prof Pieter WA Meyer

Ass. Professor and HoD

Prof PWA Meyer
Head of Department: Immunology
ResCom appointed Biostatistician
University Pretoria

Room 5-40, Level 5, Pathology Building
University of Pretoria, Private Bag X323
Pretoria 0001, South Africa
Tel +27 (0)12 319-2977
Fax +27 (0) 12 323 0732
Email name.pieter.meyer@up.ac.za
www.up.ac.za

Fakulteit Gesondheidswetenskappe
Departement Immunologie
Lefapha la Disaense tša Maphelo
Kgoro ya Immunolotši

Appendix B: MSc committee approval letters

UNIVERSITEIT VAN PRETORIA
UNIVERSITY OF PRETORIA
YUNIBESITHI YA PRETORIA

MSc Committee
School of Medicine
Faculty of Health Sciences

14 October 2021

Dr I van den Bout
Department of Physiology
Faculty of Health Sciences

Dear Dr,

Ms AL Marais, Student no 17180717

Please receive the following comments with reference to the MSc Committee submission of the abovementioned student:

Student name	Ms AL Marais	**Student number**	17180717
Name of study leader	Dr I van den Bout		
Department	Physiology		
Title of MSc	**New approved title: Assessing the role of the KISS1 receptor in breast cancer cell behaviour with the use of CRISPR-mediated gene editing** Assessing the role of KISS1R in breast cancer cell behaviour with the use of CRISPR mediated gene editing		
Date of first submission	29 September 2021		
Comments to study leader September 2021	• Please revise the title…use KISS1 receptor, rather than KISS1R. Please submit an amended MSc form. • Please revise references; should be complete (not *et al.*) and format should be consistent. • Please submit a declaration of originality. • Please correct all typographical errors. • Bacterial names and restriction enzyme names should be italicised. • Please ensure that it is clear how each objective will be achieved. • Please check spacing throughout the document. • Update timeline: submission to MSc, ethics, etc. • Include manufacturer's details for all reagents and instruments. • Include a data capturing sheet. • Revise the authorship table; be specific, indicate first author, co-author & senior author		
October 2021	• Thank you for submitting the revised protocol and requested documents.		

MSc Committee, School of Medicine
Faculty of Health Sciences
University of Pretoria,
Private Bag X323
Pretoria 0001, South Africa
Tel +27 (0)12 319 2325
Fax +27 (0)12 323 0732

Fakulteit Gesondheidswetenskappe
Lefapha la Disaense tša Maphelo

Decision	This protocol has been provisionally approved. Please submit the revised protocol to ethics, and supply the MSc committee with proof of acceptance. The internal and external examiners can be nominated and submitted to the MSc Committee six months prior to submission of the dissertation. Please ensure that the CV of the examiners includes: supervision, examination and publication records

Yours sincerely

Prof Marleen Kock
Chair: MSc Committee

Faculty of Health Sciences
Fakulteit Gesondheidswetenskappe
Lefapha la Disaense tša Maphelo

UNIVERSITEIT VAN PRETORIA
UNIVERSITY OF PRETORIA
YUNIBESITHI YA PRETORIA

MSc Committee
School of Medicine
Faculty of Health Sciences

17 November 2021

Dr I van den Bout
Department of Physiology
Faculty of Health Sciences

Dear Dr,

Ms AL Marais, Student no 17180717

Please receive the following comments with reference to the MSc Committee submission of the abovementioned student:

Student name	Ms AL Marais	**Student number**	17180717
Name of study leader	Dr I van den Bout		
Department	Physiology		
Title of MSc	**New approved title: Assessing the role of the KISS1 receptor in breast cancer cell behaviour with the use of CRISPR-mediated gene editing** Assessing the role of KISS1R in breast cancer cell behaviour with the use of CRISPR mediated gene editing		
Date of first submission	29 September 2021		
October 2021	• Thank you for submitting the revised protocol and requested documents.		
November 2021	• Thank you for submitting the ethics clearance certificate.		
Decision	This protocol has been approved. Ethics approval has been obtained. The internal and external examiners can be nominated and submitted to the MSc Committee six months prior to submission of the dissertation. Please ensure that the CV of the examiners includes: supervision, examination and publication records		

Yours sincerely

Prof Marleen Kock
Chair: MSc Committee

MSc Committee, School of Medicine
Faculty of Health Sciences
University of Pretoria,
Private Bag X323
Pretoria 0001, South Africa
Tel +27 (0)12 319 2325
Fax +27 (0)12 323 0732

Fakulteit Gesondheidswetenskappe
Lefapha la Disaense tša Maphelo

Appendix C: Ethical clearance letter

UNIVERSITEIT VAN PRETORIA
UNIVERSITY OF PRETORIA
YUNIBESITHI YA PRETORIA

Faculty of Health Sciences

Institution: The Research Ethics Committee, Faculty Health Sciences, University of Pretoria complies with ICH-GCP guidelines and has US Federal wide Assurance.

- FWA 00002567, Approved dd 22 May 2002 and Expires 03/20/2022.
- IORG #: IORG0001762 OMB No. 0990-0279 Approved for use through February 28, 2022 and Expires: 03/04/2023.

Faculty of Health Sciences **Research Ethics Committee**

10 November 2021

Approval Certificate
New Application

Dear Miss AL Marais

Ethics Reference No.: 608/2021
Title: Assessing the role of the KISS1 receptor in breast cancer cell behaviour with the use of CRISPR-mediated gene editing

The **New Application** as supported by documents received between 2021-10-20 and 2021-11-10 for your research, was approved by the Faculty of Health Sciences Research Ethics Committee on 2021-11-10 as resolved by its quorate meeting.

Please note the following about your ethics approval:

- Ethics Approval is valid for 1 year and needs to be renewed annually by 2022-11-10.
- Please remember to use your protocol number (608/2021) on any documents or correspondence with the Research Ethics Committee regarding your research.
- Please note that the Research Ethics Committee may ask further questions, seek additional information, require further modification, monitor the conduct of your research, or suspend or withdraw ethics approval.

Ethics approval is subject to the following:

- The ethics approval is conditional on the research being conducted as stipulated by the details of all documents submitted to the Committee. In the event that a further need arises to change who the investigators are, the methods or any other aspect, such changes must be submitted as an Amendment for approval by the Committee.

We wish you the best with your research.

Yours sincerely

On behalf of the FHS REC, Professor Werdie (CW) Van Staden
MBChB, MMed(Psych), MD, FCPsych(SA), FTCL, UPLM
***Chairperson**: Faculty of Health Sciences Research Ethics Committee*

The Faculty of Health Sciences Research Ethics Committee complies with the SA National Act 61 of 2003 as it pertains to health research and the United States Code of Federal Regulations Title 45 and 46. This committee abides by the ethical norms and principles for research, established by the Declaration of Helsinki, the South African Medical Research Council Guidelines as well as the Guidelines for Ethical Research: Principles Structures and Processes, Second Edition 2015 (Department of Health)

Research Ethics Committee
Room 4-60, Level 4, Tswelopele Building
University of Pretoria, Private Bag x323
Gezina 0031, South Africa
Tel +27 (0)12 356 3084
Email: deepeka.behari@up.ac.za
www.up.ac.za

Fakulteit Gesondheidswetenskappe
Lefapha la Disaense tša Maphelo

Appendix D: Turnitin report

turnitin

Digital Receipt

This receipt acknowledges that Turnitin received your paper. Below you will find the receipt information regarding your submission.

The first page of your submissions is displayed below.

Submission author:	AL (Alex) Marais
Assignment title:	Any document
Submission title:	MSc Dissertation
File name:	AL_Marais_MSc_Dissertation.docx
File size:	13.19M
Page count:	95
Word count:	21,118
Character count:	116,817
Submission date:	09-Feb-2023 02:03PM (UTC+0200)
Submission ID:	2010039418

UNIVERSITEIT VAN PRETORIA
UNIVERSITY OF PRETORIA
YUNIBESITHI YA PRETORIA

Assessing the role of the KISS1 receptor in breast cancer behaviour with the use of CRISPR-mediated gene editing

By

Alex Leah Marais

Submitted in partial fulfilment of the requirements for the Master of Science degree in

Human Physiology

in the

Department of Physiology

Faculty of Health Sciences

UNIVERSITY OF PRETORIA

2023

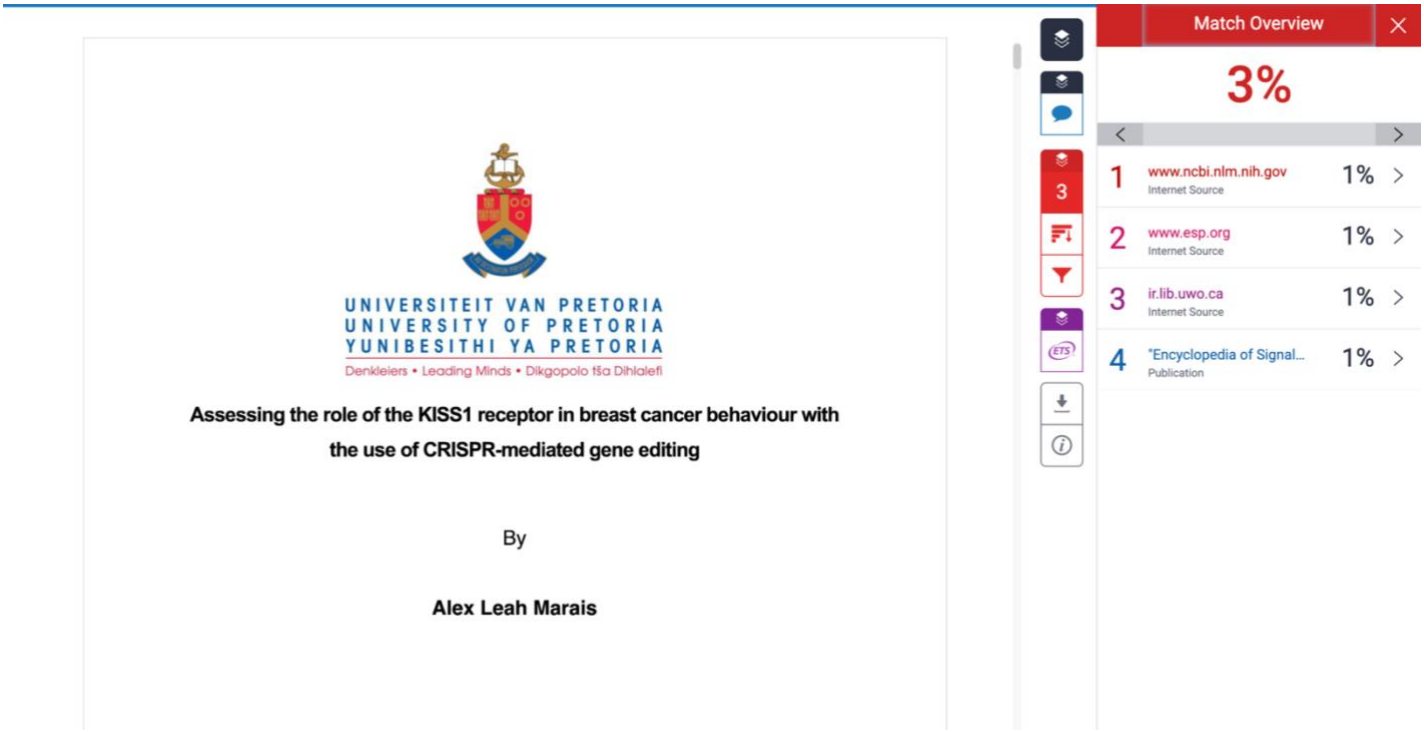
UNIVERSITEIT VAN PRETORIA
UNIVERSITY OF PRETORIA
YUNIBESITHI YA PRETORIA
Denkleiers • Leading Minds • Dikgopolo tša Dihlalefi
Assessing the role of the KISS1 receptor in breast cancer behaviour with the use of CRISPR-mediated gene editing
By
Alex Leah Marais
Match Overview
3%
1 www.ncbi.nlm.nih.gov Internet Source 1%
2 www.esp.org Internet Source 1%
3 ir.lib.uwo.ca Internet Source 1%
4 "Encyclopedia of Signal... Publication 1%